Cours du 12 décembre 2011

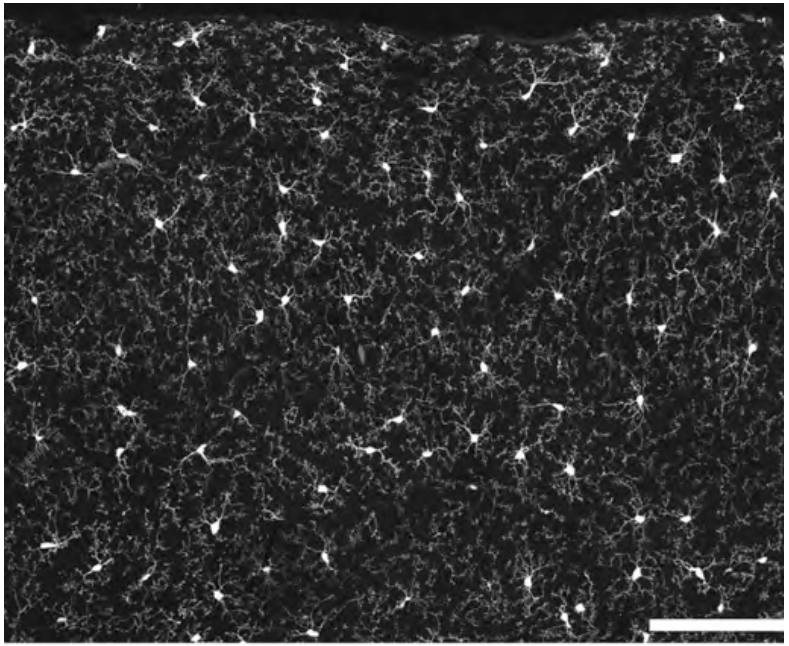

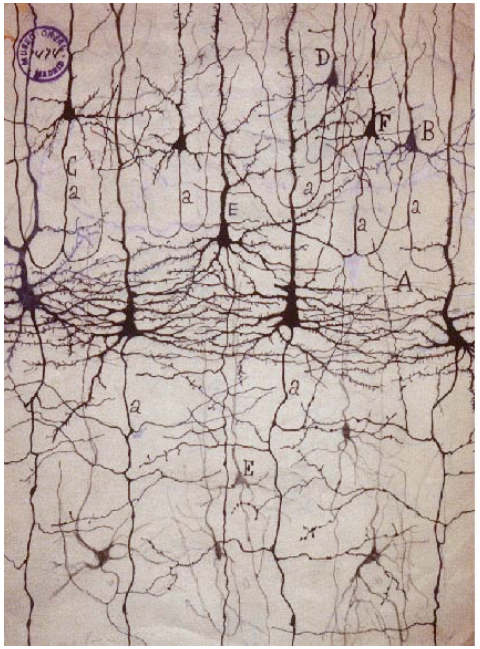
D
F
B
C
a
E
A


I
II
III
IVA
IVB
IVCa
IVCb
V
VI

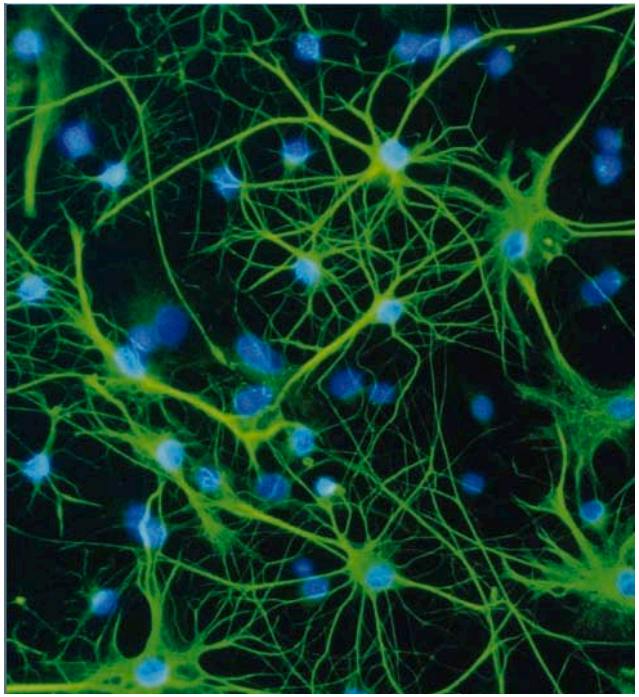

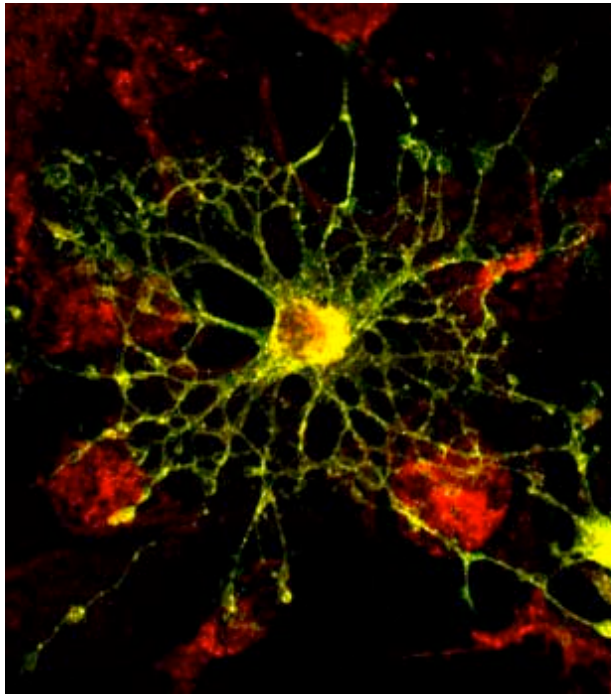

Dynamics of CNS barriers: evolution, differentiation, and modulation

Abbott N

Cell Mol Neurobiol
2005 vol. 25 (1) pp. 5-23

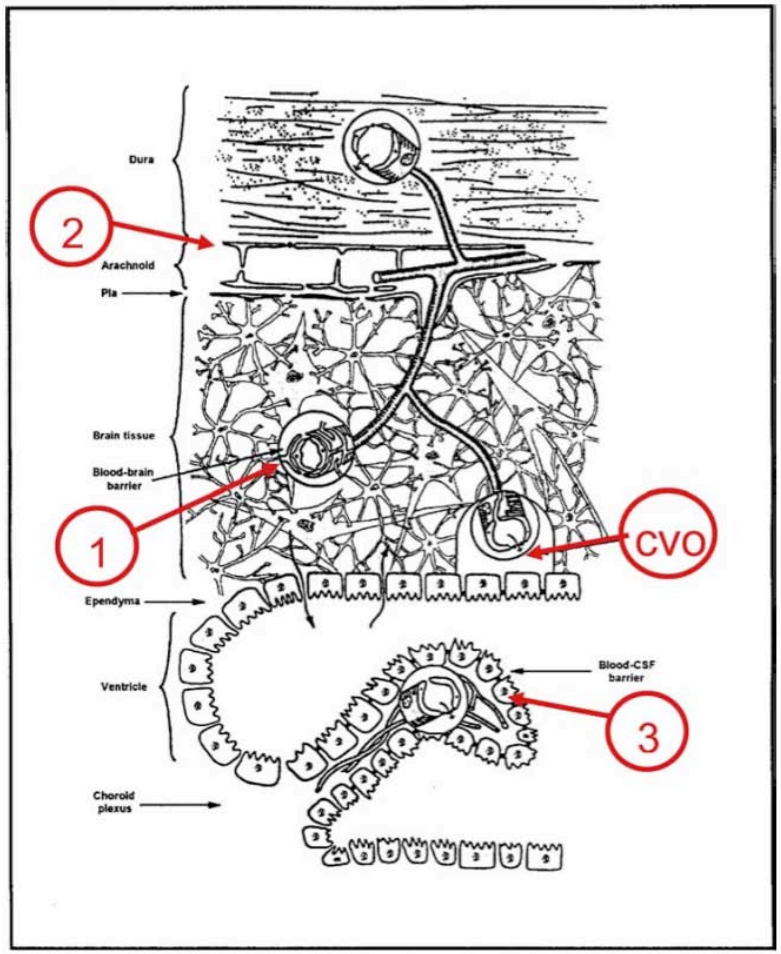

Fig. 1. Location of barrier sites in the CNS. Barriers are present at three main sites: (1) the brain endothelium forming the blood–brain barrier (BBB), (2) the arachnoid epithelium forming the middle layer of the meninges, and (3) the choroid plexus epithelium which secretes cerebrospinal fluid (CSF). In each site, the physical barrier is caused by tight junctions that reduce the permeability of the paracellular (intercellular cleft) pathway. In circumventricular organs (CVO), containing neurons specialized for neurosecretion and/or chemosensitivity, the endothelium is leaky. This allows tissue-blood exchange, but as these sites are separated from the rest of the brain by an external glial barrier, and from CSF by a barrier at the ependyma, CVOs do not form a leak across the BBB. (Based on Segal and Zlokovic, 1990), modified by A. Reichel (with permission).

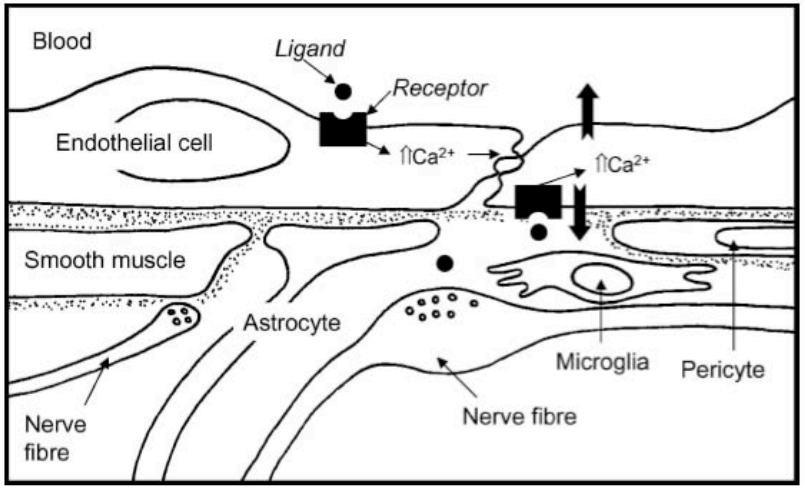

Fig. 2. Cell types associated with the brain endothelium forming the blood–brain barrier. Pericytes are enclosed within the endothelial basal lamina and form the closest associations with endothelium. The end-feet of astrocytic glial cells are apposed to the outer surface of the basal lamina. In the perivascular space are found microglia, the synaptic terminals and boutons of nerve fibres, and (in arterioles), smooth muscle cells. In the larger vessels, cells of the meninges form a perivascular cuff or sheath projecting down from the brain surface, and demarcating the Virchow-Robin space (not shown). Agents can influence endothelial function by ligand-receptor interaction, from the blood or the brain side. Some receptors are coupled to elevation of intracellular [Ca^{2+}]. The heavy arrows indicate the ability of the endothelium to release agents to the blood or brain side following receptor activation, as part of their 'effector' function.

News from the brain: the GPR124 orphan receptor directs brain-specific angiogenesis

Science Translational Medicine
2010 vol. 2 (58) pp. 58ps53

Dejana E, Nyqvist D

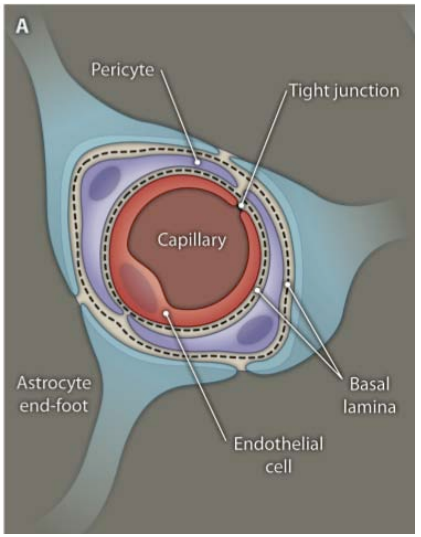

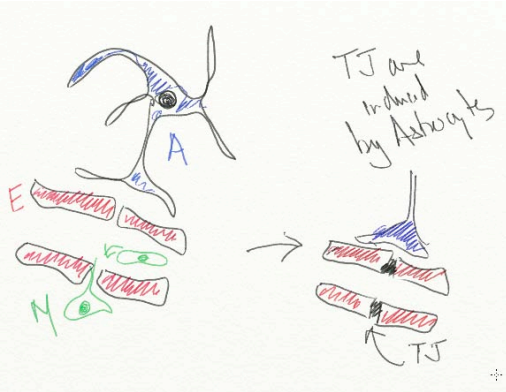

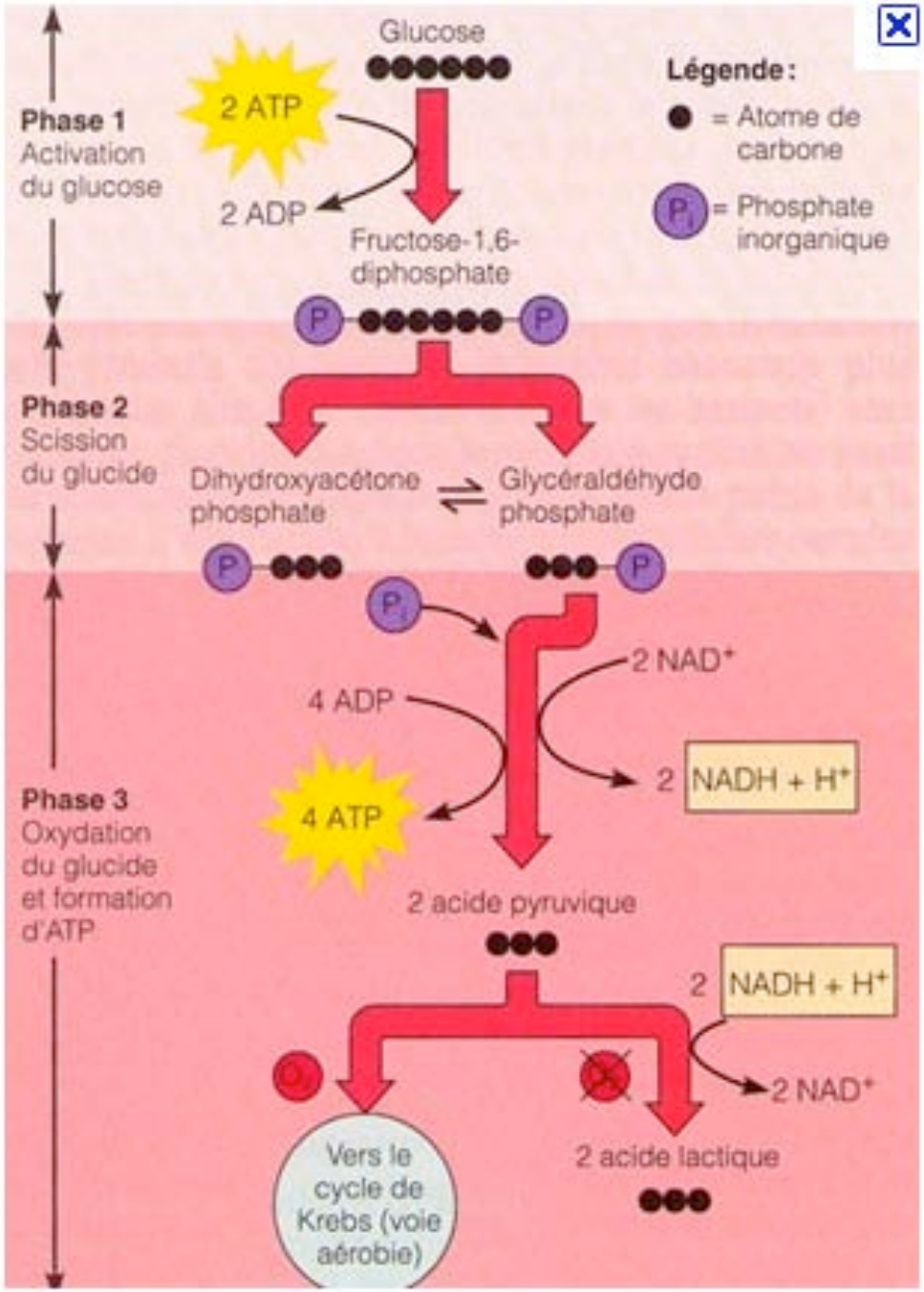

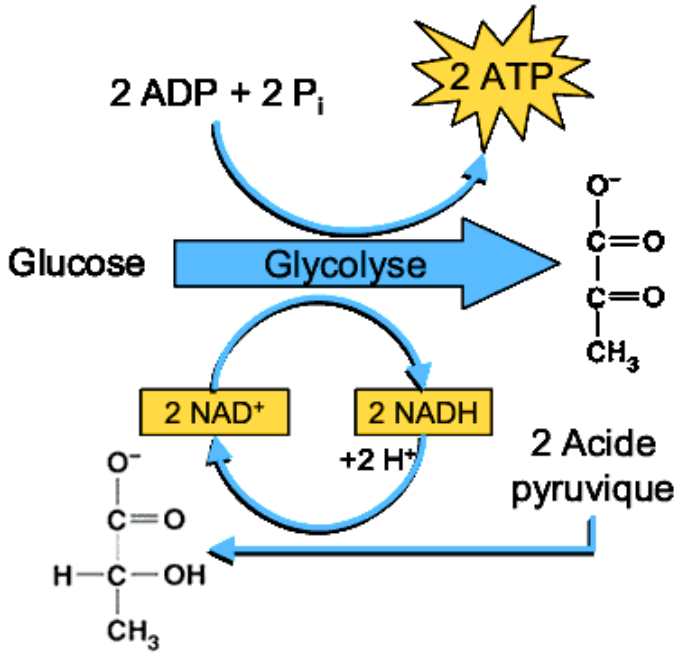

2 Acide lactique

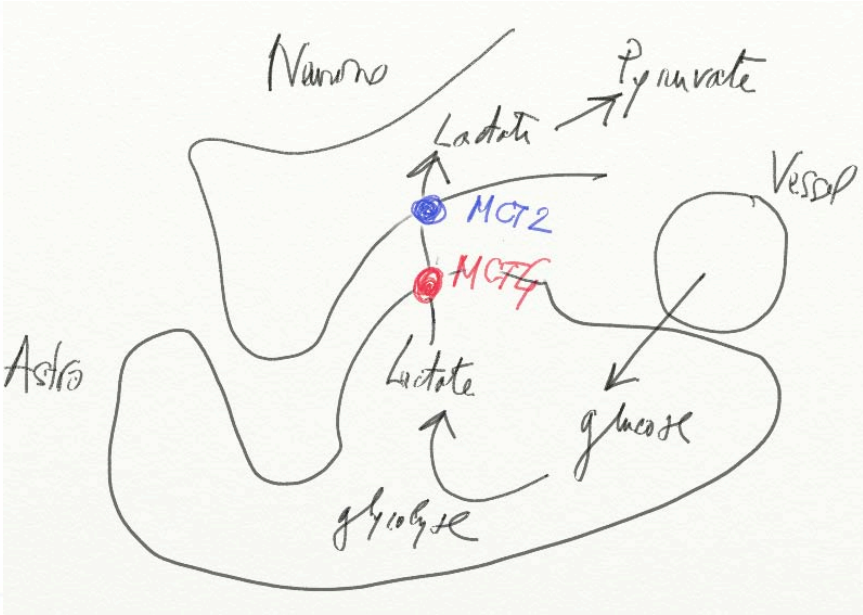

Fragile balance: RNA editing tunes the synapse

Bassell G

Nature Neuroscience 14, 1492 (2011). doi: 10.1038/nn.2982

Nature Neuroscience
2011 vol. 14 (12) pp. 1492–1494

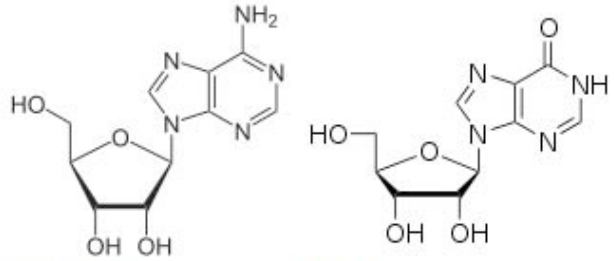

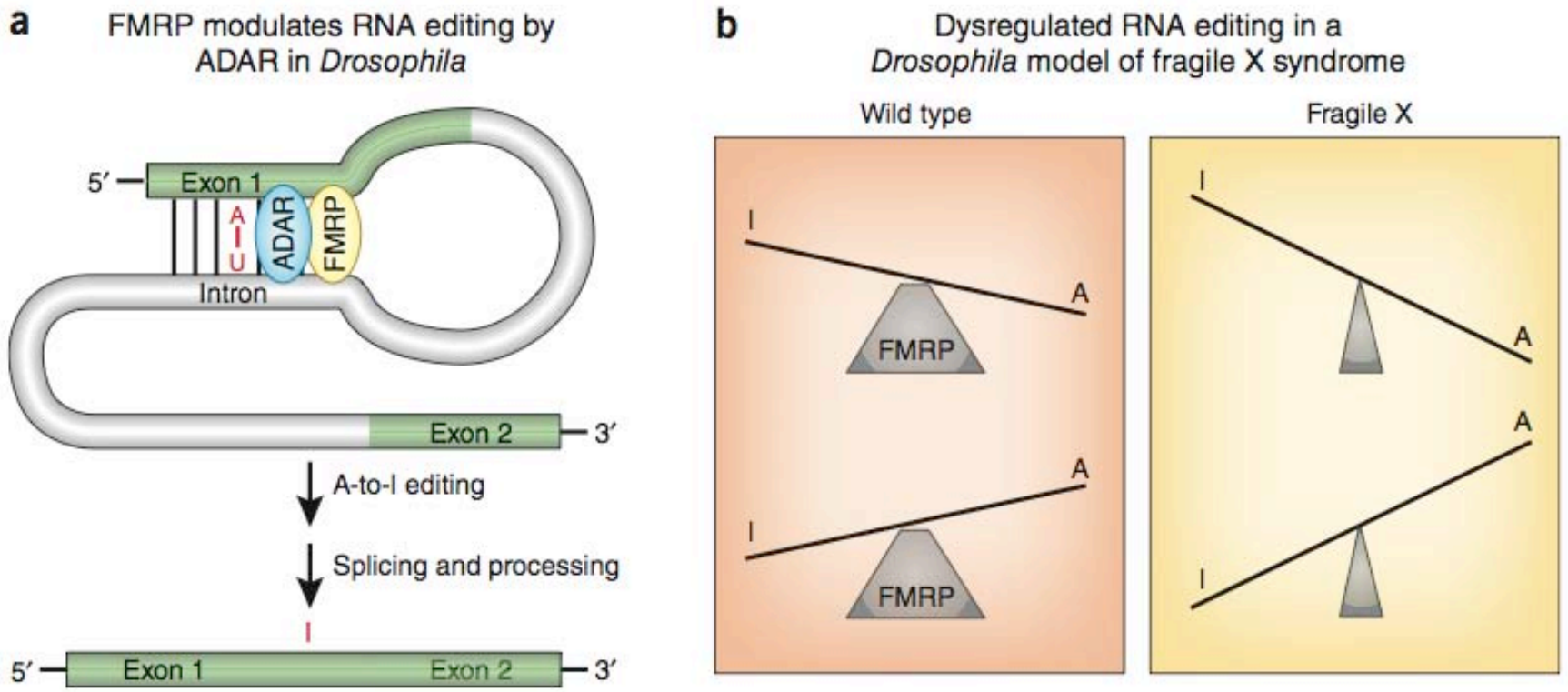

Katie Vicari

Figure 1 Regulation of A-to-I RNA editing by FMRP in *Drosophila*. (**a**) The data of Bhogal *et al.*[2], together with other studies, suggest a model in which ADAR and FMRP cooperate in the nucleus to regulate ADAR activity, possibly on double-stranded RNA targets comprising exonic and intronic sequences. (**b**) In wild-type neurons (left), the amount of RNA editing is tightly controlled or fine-tuned by FMRP, whereas RNA editing is imbalanced and dysregulated in fragile X syndrome (right), as a result of a loss of control at the fulcrum.

Regeneration, repair and remembering identity: the three Rs of *Hox* gene expression

Kevin C. Wang[1,2], Jill A. Helms[3] and Howard Y. Chang[1]

Trends in Cell Biology Vol.19 No.6

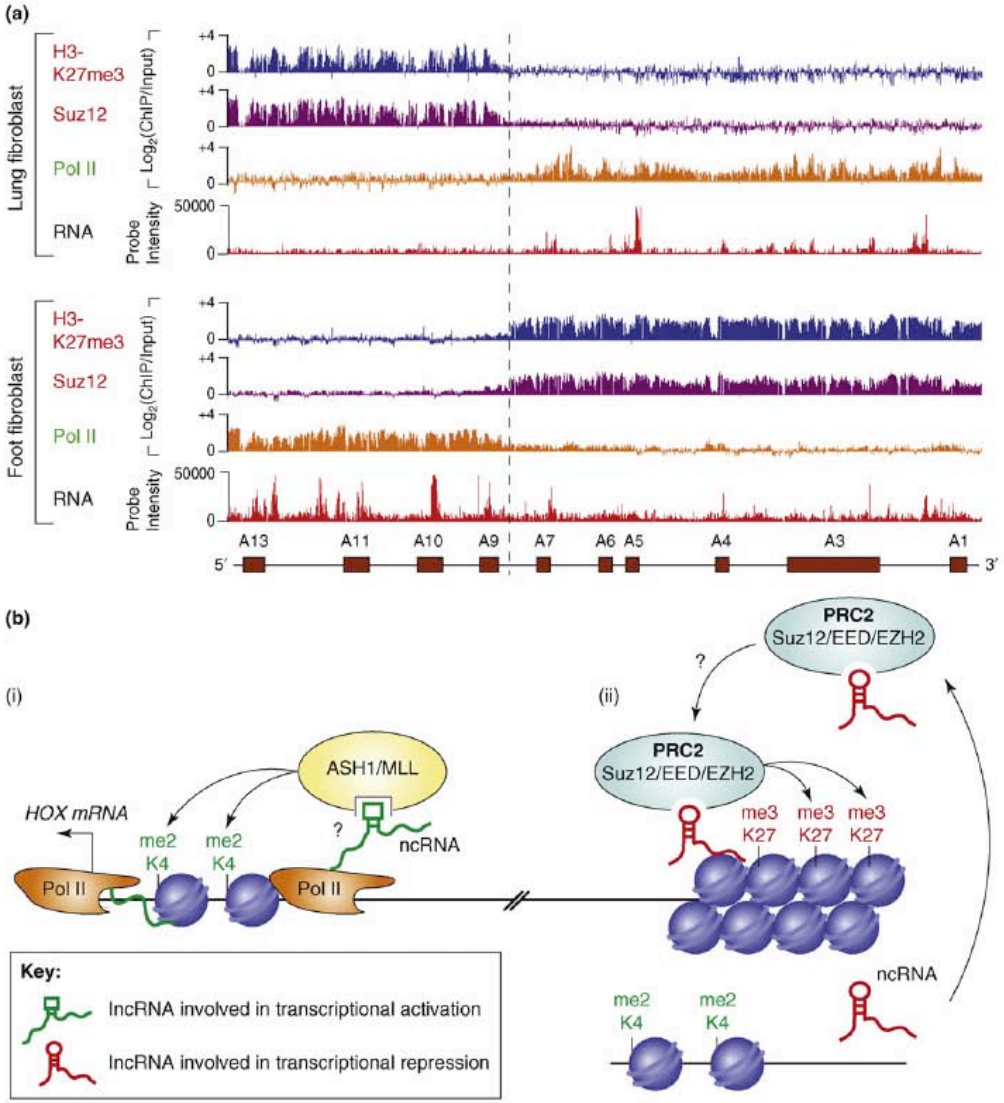

Repatterning in amphibian limb regeneration: A model for study of genetic and epigenetic control of organ regeneration

Nayuta Yakushiji, Hitoshi Yokoyama, Koji Tamura*

Seminars in Cell & Developmental Biology 20 (2009) 565–574

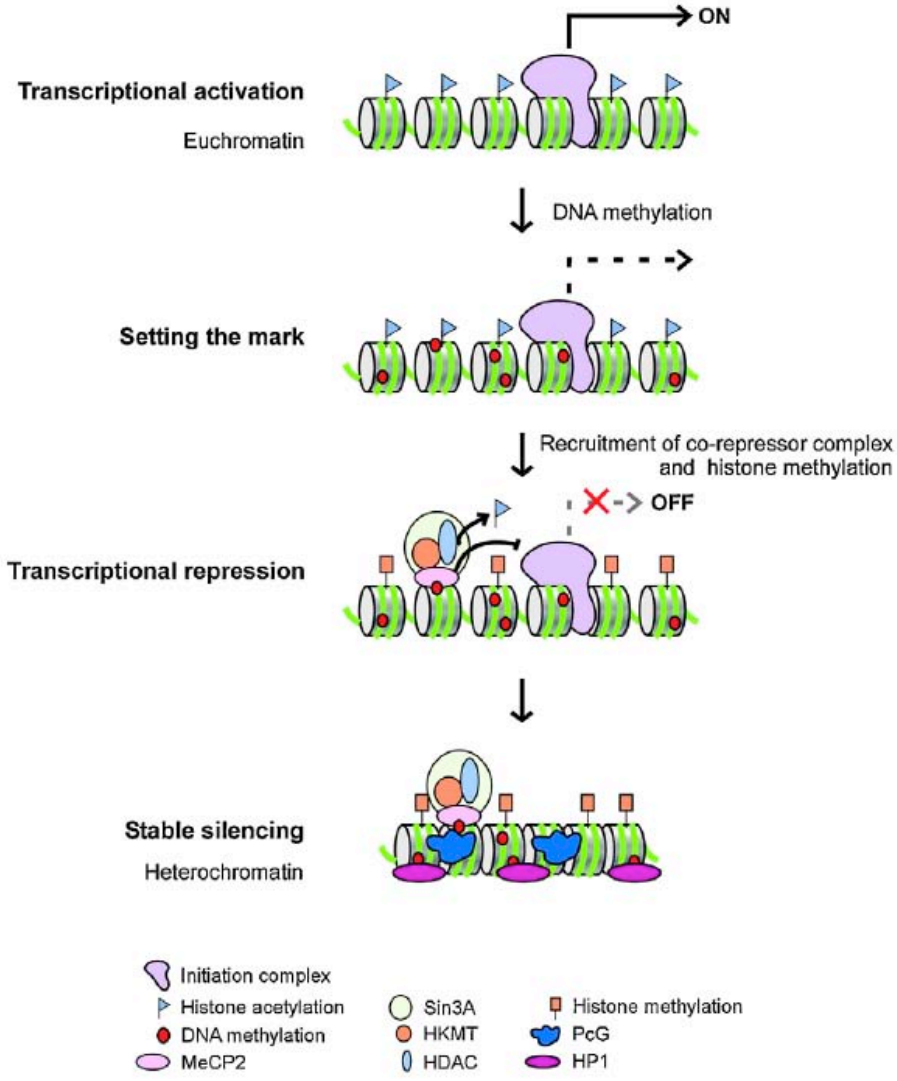

Astrocyte-neuron lactate transport is required for long-term memory formation

Suzuki A, Stern SA, Bozdagi O, Huntley GW, Walker RH, Magistretti PJ, Alberini CM

Cell
2011 vol. 144 (5) pp. 8...

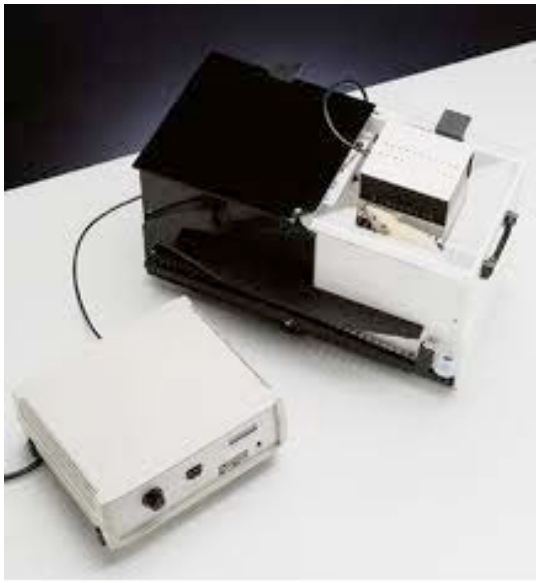

Day 1: Training

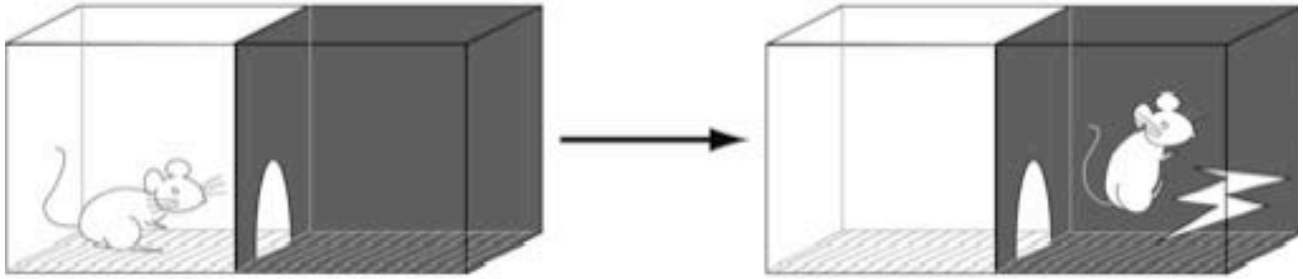

Mice usually go into the dark compartment because they prefer dark environment. Once entered, however, a foot-shock is delivered through the grid floor.

Day 2: Memory test

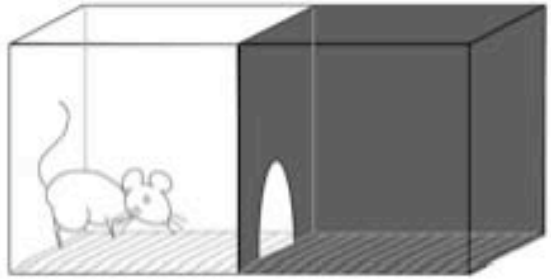

Normal mice never go into the dark compartment again.

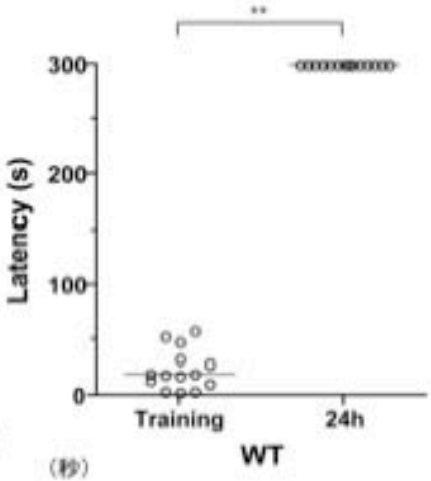

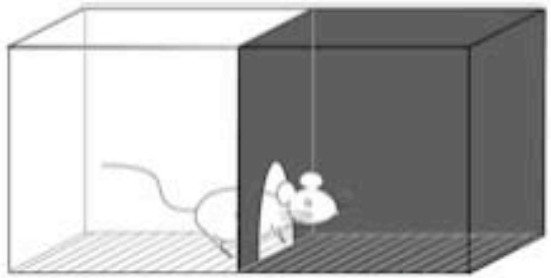

CaMKIIα(K42R) mice easily go into the dark compartment.

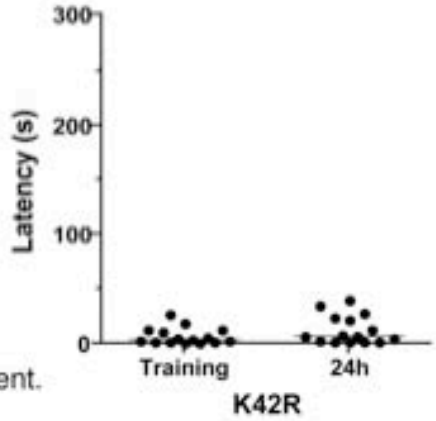

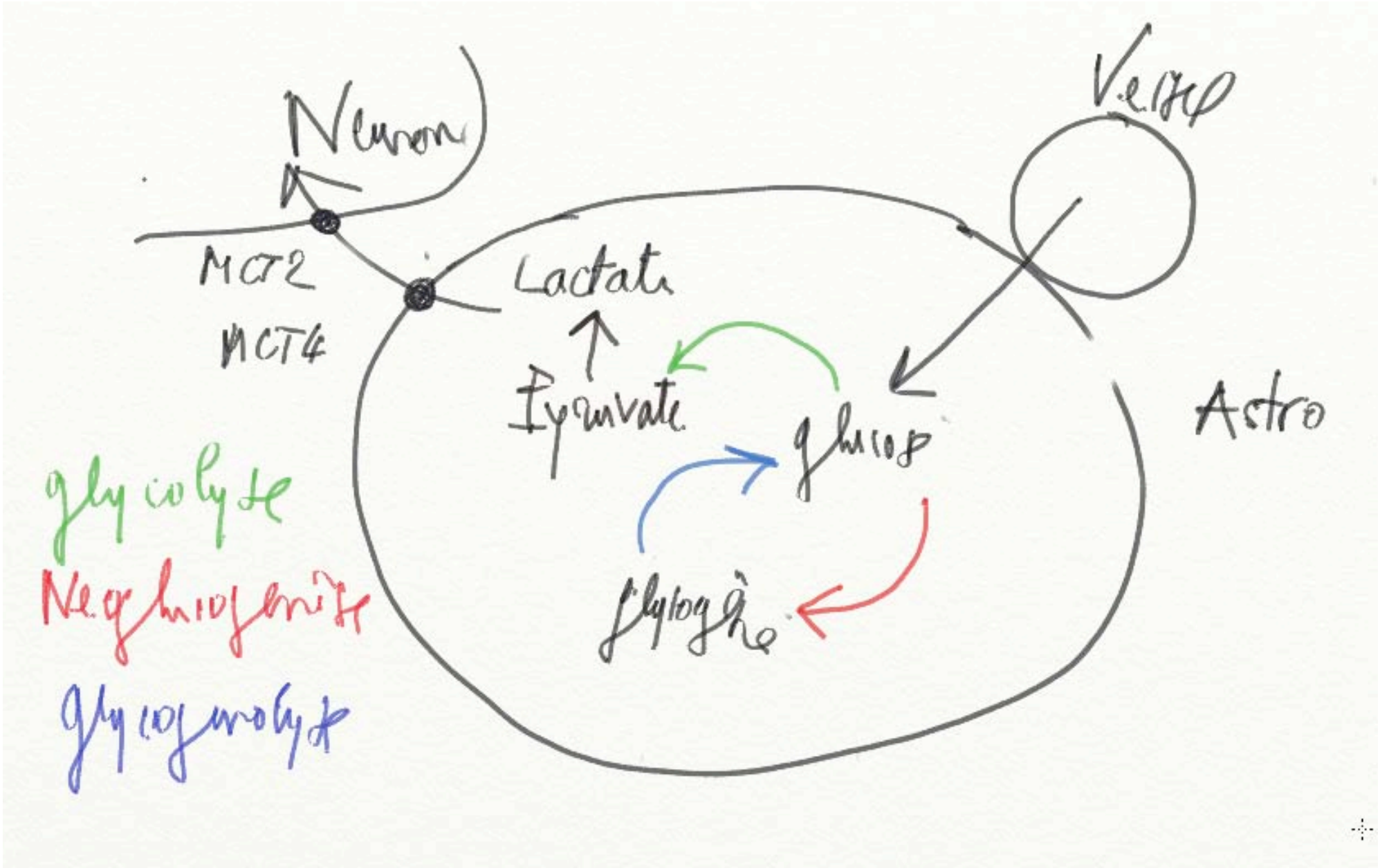
Neuron
MCT2
MCT4
Lactate
Pyruvate
Astro
glycolyte
Neoglucogenèse
glycogénolyse

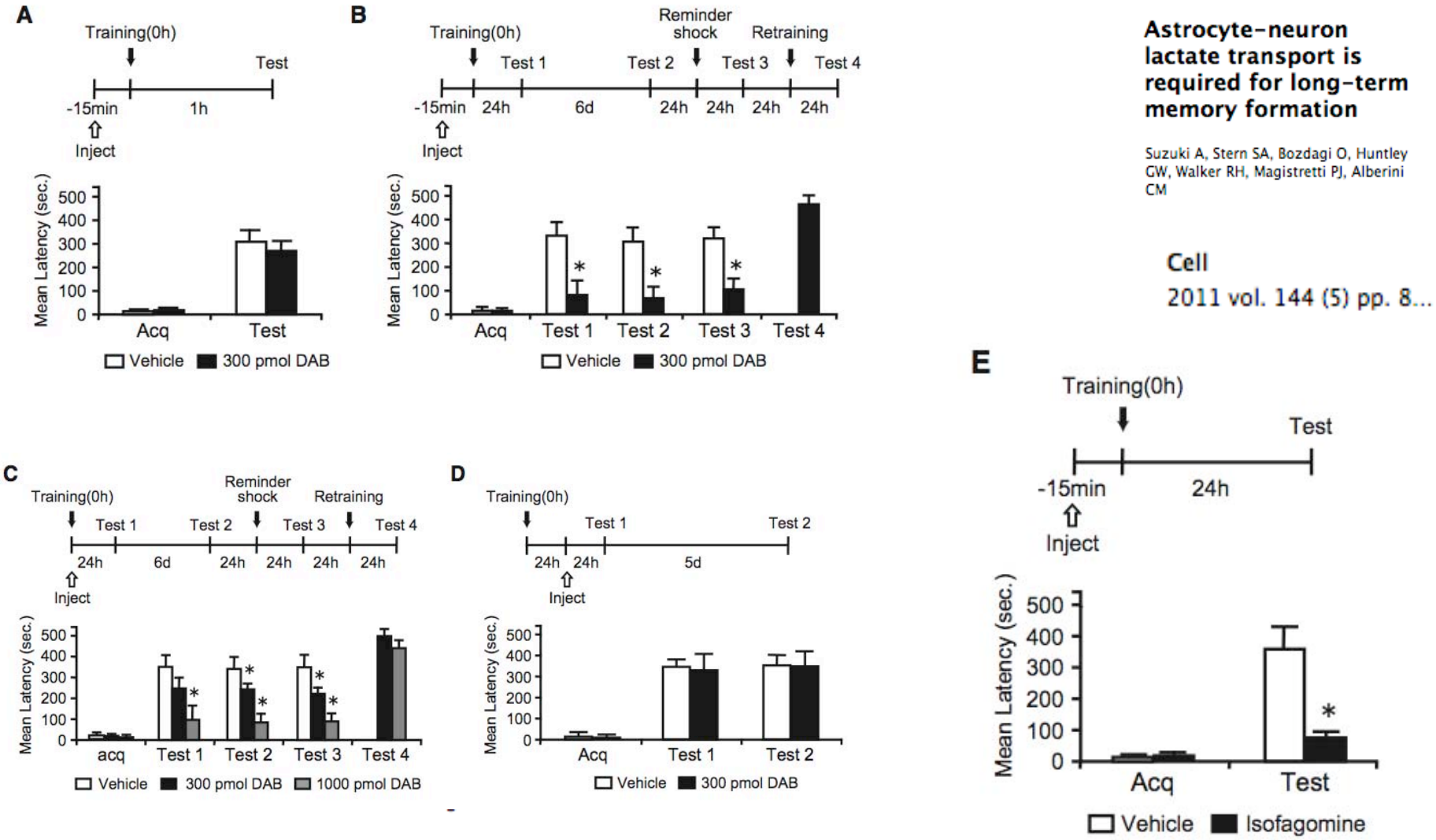

Astrocyte-neuron lactate transport is required for long-term memory formation

Suzuki A, Stern SA, Bozdagi O, Huntley GW, Walker RH, Magistretti PJ, Alberini CM

Cell
2011 vol. 144 (5) pp. 8...

Figure 1. DAB and Isofagomine Disrupt Long-Term Memory

Acquisition (Acq) and retention are expressed as mean latency ± SEM (in seconds, sec). Latency scores, n and detailed statistic are reported in Table S1. See also Figure S1.

(A) Hippocampal injections of DAB 15 min before IA training had no effect on short-term memory tested at 1 hr after training (n = 7/group).

(B and C) Hippocampal injections of DAB 15 min before ([B] n = 11/group) or immediately after training ([C] n = 7–9/group) disrupted long-term memory at 24 hr (Test 1). The disruption persisted 7 days after training (Test 2), and memory did not recover after a reminder shock (Test 3). DAB-injected rats had normal retention after retraining (Test 4).

(D) Hippocampal injections of DAB 24 hr after IA training did not affect long-term memory (n = 8/group).

(E) Hippocampal injections of isofagomine 15 min before training disrupted long-term memory (n = 8-9/group). *p < 0.05.

Astrocyte-neuron lactate transport is required for long-term memory formation

Suzuki A, Stern SA, Bozdagi O, Huntley GW, Walker RH, Magistretti PJ, Alberini CM

Cell
2011 vol. 144 (5) pp. 8...

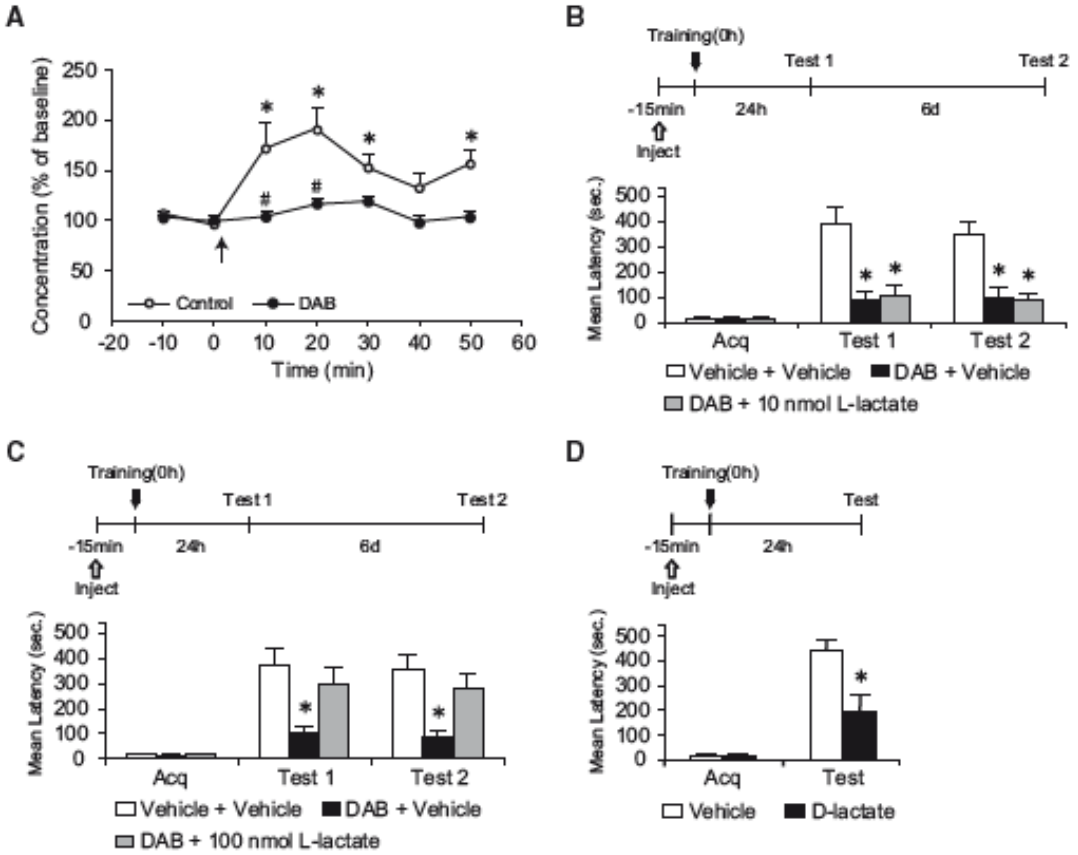

Figure 2. L-Lactate Rescues the DAB-Induced Memory Impairment

Lactate concentration, latency scores, n and detailed statistic are reported in Table S2.

(A) Dorsal hippocampal extracellular lactate in freely moving rats infused with either vehicle or DAB. Baseline was collected for 20 min before training (0 min, ↑) and continued for 50 min. Training resulted in a significant increase in lactate levels compared to baseline (*$p < 0.05$) that was completely blocked by DAB (#$p < 0.05$). Data are expressed as % of baseline ± SEM (mean of the first 2 samples set 100%). See also Figure S2.

(B–D) Acquisition (Acq) and retention are expressed as mean latency ± SEM (in seconds, sec).

(B and C) Hippocampal injection of DAB or vehicle in combination with 10 nmol (B, n = 7/group), 100 nmol L-lactate (C, n = 12/group) or vehicle were performed 15 min before training and memory was tested at 24 hr. 100 nmol but not 10 nmol of L-lactate rescued the memory impairment by DAB (Test 1). The effect persisted at 7 days after training (Test 2).

(D) Hippocampal injections of D-lactate 15 min before training disrupted long-term memory (n = 7–8/group). *$p < 0.05$.

Astrocyte-neuron lactate transport is required for long-term memory formation

Suzuki A, Stern SA, Bozdagi O, Huntley GW, Walker RH, Magistretti PJ, Alberini CM

Cell
2011 vol. 144 (5) pp. 8...

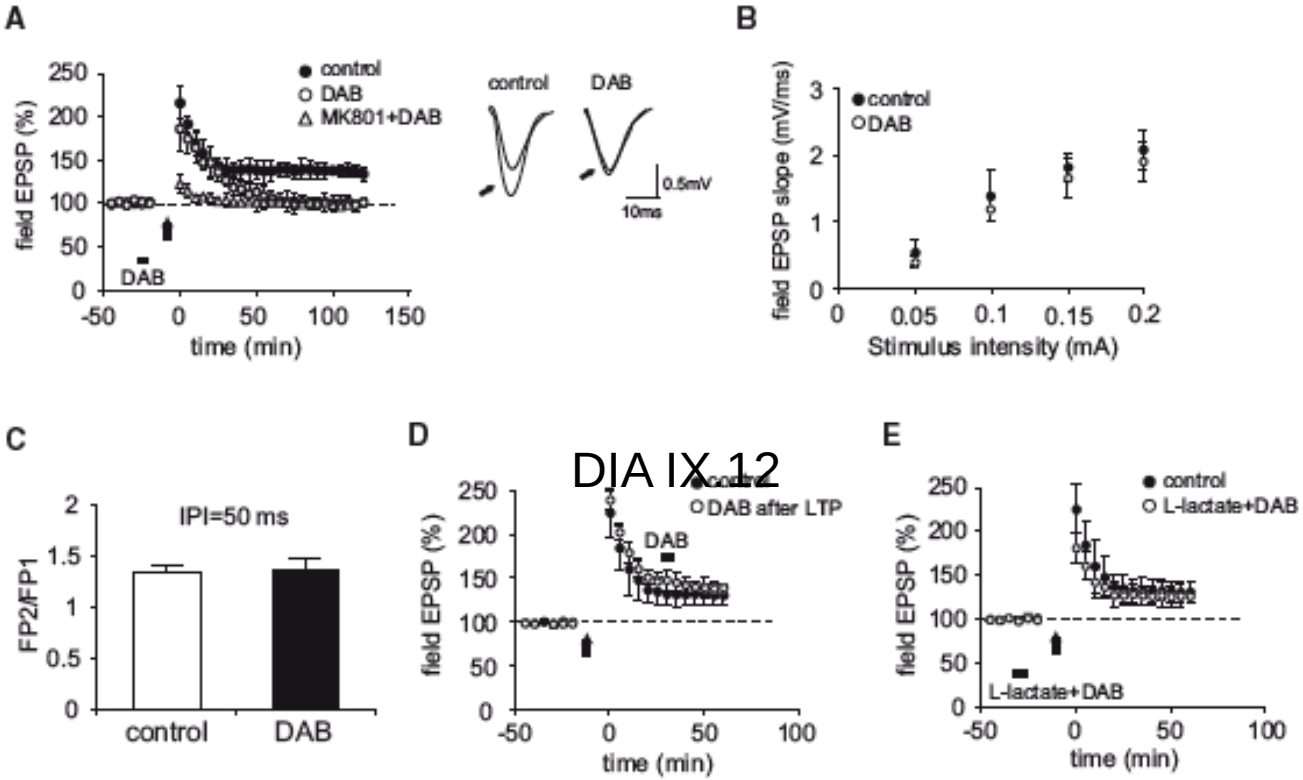

DIA IX.12

Figure 3. DAB Impairs In Vivo Hippocampal LTP and the Impairment Is Rescued by L-Lactate

(A) Average Field EPSP data recorded for 120 min posttetanus shows that DAB injection (bar) before high frequency stimulation (arrow) blocks LTP ($p < 0.05$ versus controls at 120 min, n = 4/group). LTP is abolished in animals receiving an intraperitoneal injection of the N-methyl-D-aspartate (NMDA) receptor antagonist MK-801 (3mg/kg) 30 min prior to tetanus (open triangles). Inset: Representative EPSP traces were recorded before and 120 min after (indicated by arrows) LTP induction. Left panel, control; right panel, in the presence of DAB.

(B and C) No effect on the relationship between stimulus strength and the size of the postsynaptic response (input-output relationship, B, n = 4/group, $p > 0.05$) or paired-pulse facilitation (PPF, C, n = 4/group, $p > 0.05$).

(D) DAB injected 30 min after high frequency stimulation did not affect synaptic potentiation (n = 4/group).

(E) L-lactate reversed the blocking effect of DAB on LTP (n = 4/group).

All data are expressed as mean values ± SEM.

Astrocyte-neuron lactate transport is required for long-term memory formation

Cell
2011 vol. 144 (5) pp. 8...

Suzuki A, Stern SA, Bozdagi O, Huntley GW, Walker RH, Magistretti PJ, Alberini CM

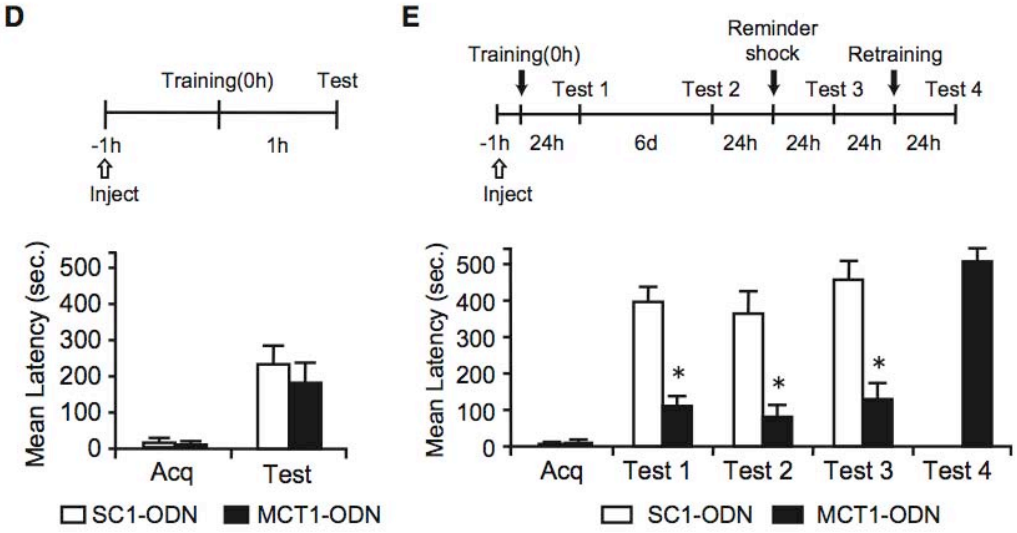

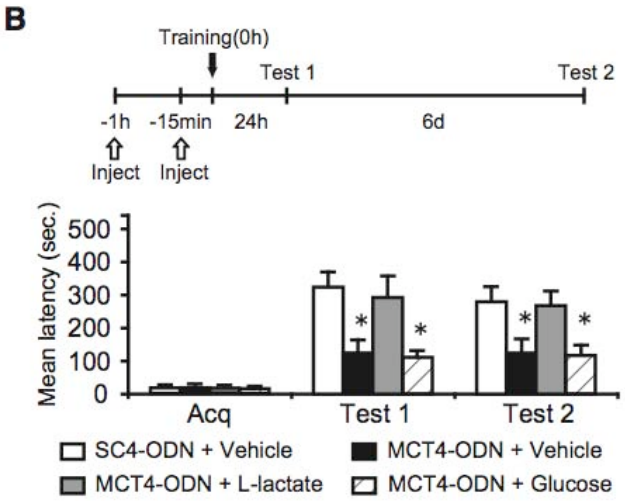

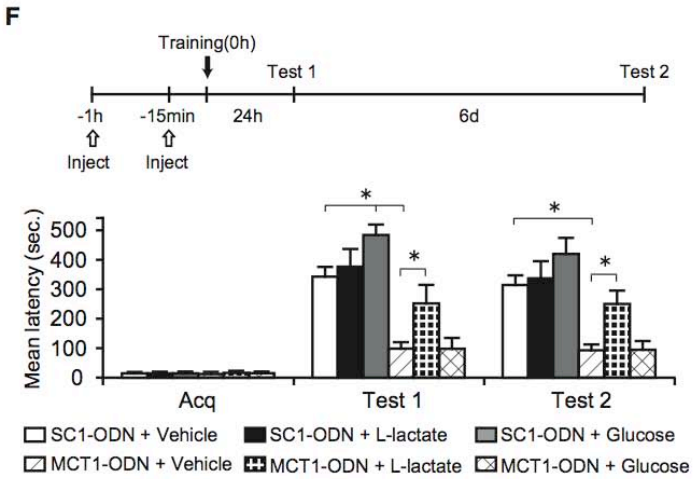

(B) Memory acquisition (acq) and retention are expressed as mean latency ± SEM (in seconds, sec). Hippocampal injection of MCT4-ODN disrupted long-term memory and L-lactate but not glucose, rescued it. MCT4- or SC4-ODN were injected 1 hr before training. L-lactate, glucose or vehicle (PBS) were injected 15 min before training. Rats were tested 24 hr after training (Test 1) and 6 days later (Test 2). (n = 10-12/group). *p < 0.05.

(D–G) Memory acquisition (acq) and retention are expressed as mean latency ± SEM (in seconds, sec).
(D) Hippocampal injections of MCT1-ODN 1 hr before training did not affect short-term memory (n = 7/group).
(E) Hippocampal injection of MCT1-ODN disrupted long-term memory. MCT1- or SC1-ODN were injected 1 hr before training and rats were tested 24 hr after training (Test 1) and 6 days later (Test 2). The memory disruption persisted at Test 2, and memory did not recover following a reminder shock (Test 3). MCT1-ODN amnesic rats showed normal retention after retraining (Test 4) (n = 10–11/group).
(F) L-lactate but not glucose rescued the memory impairment induced by blocking MCT1 expression (n = 7-13/group). MCT1- or SC1-ODN were injected 1 hr before training. L-lactate, glucose or vehicle (PBS) were injected 15 min before training. Rats were tested 24 hr after training (Test 1) and 6 days later (Test 2).

Astrocyte-neuron lactate transport is required for long-term memory formation

Cell
2011 vol. 144 (5) pp. 8...

Suzuki A, Stern SA, Bozdagi O, Huntley GW, Walker RH, Magistretti PJ, Alberini CM

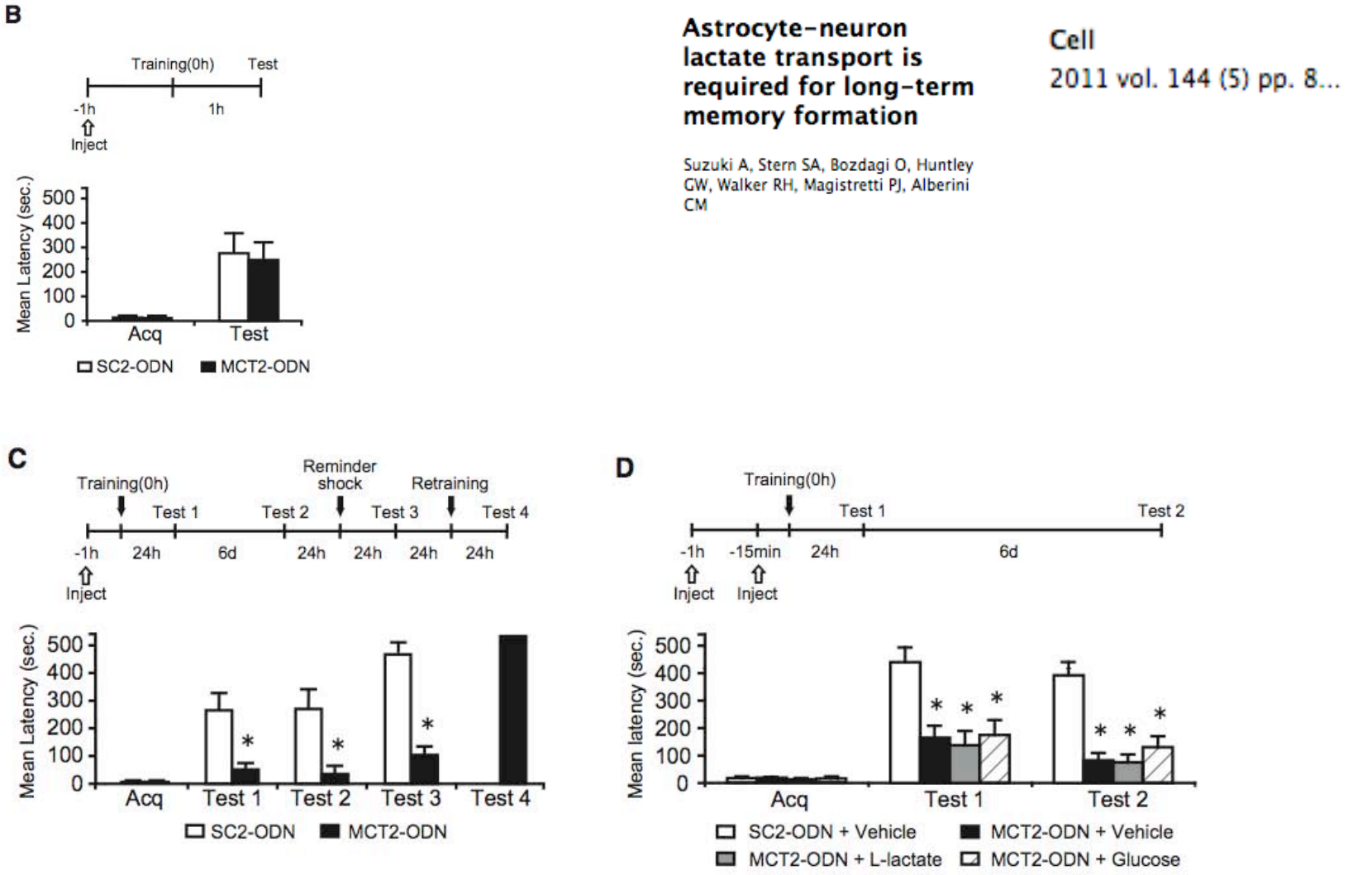

(B–D) Acquisition (acq) and retention are expressed as mean latency ± SEM (in seconds, sec).

(B) Hippocampal injections of MCT2-ODN 1 hr before training did not affect short-term memory tested 1 hr later (n = 8/group).

(C) Hippocampal injections of MCT2-ODN disrupted long-term memory. MCT2- or SC2-ODN were injected 1 hr before training. Rats were tested 24 hr after training (Test 1) and 6 days later (Test 2). The memory disruption persisted at Test 2, and memory did not recover following a reminder foot shock (Test 3). The amnesic rats that received the MCT2-ODN showed normal retention after retraining (Test 4) (n = 8/group).

(D) Neither L-lactate nor glucose rescued the memory impairment induced by MCT2 disruption (n = 6-8/group). MCT2- or SC2-ODN were injected 1 hr before training. L-lactate, glucose or vehicle (PBS) were injected 15 min before training. Rats were tested 24 hr after training (Test 1) and 6 days later (Test 2). *$p < 0.05$.

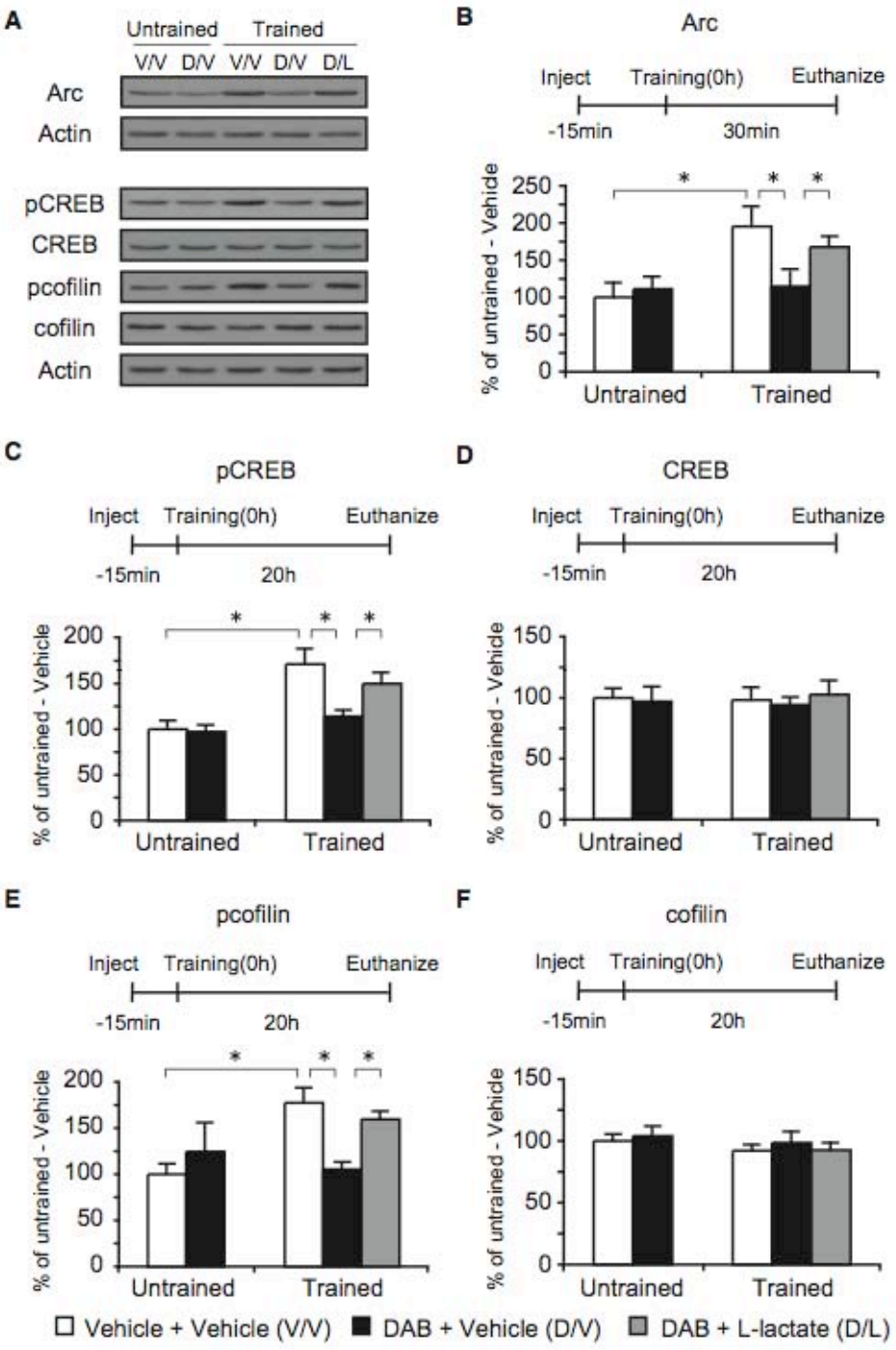

Astrocyte-neuron lactate transport is required for long-term memory formation

Suzuki A, Stern SA, Bozdagi O, Huntley GW, Walker RH, Magistretti PJ, Alberini CM

Cell
2011 vol. 144 (5) pp. 8...

Figure 7. Training-Induced Increase of Arc, pCREB, and Pcofilin Are Completely Blocked by DAB and Significantly Rescued by L-Lactate

Mean %, n, and detailed statistic are reported in Table S6.

(A–F) Examples (A) and densitometric western blot analysis of Arc (B), pCREB (C), CREB (D), pcofilin (E), and cofilin (F) performed on dorsal hippocampal extracts from trained and untrained rats injected 15 min before training with vehicle, DAB+vehicle or DAB+L-lactate and euthanized 30 min (for Arc) or 20 hr (for all other markers) after training. See also Figure S3.

Arc (B), pCREB (C), and pcofilin (E) expression were significantly increased after training. This increase was completely blocked by DAB and rescued by L-lactate. There is no change in expression of CREB (D) and cofilin (F) across samples (n = 4–7/group).

Data are expressed as mean percentage ± SEM of untrained, vehicle-injected control (100%) mean values. All proteins values were normalized to those of actin. *$p < 0.05$.

Cellular scaling rules for primate brains

Proc Natl Acad Sci USA
2007 vol. 104 (9) pp. 3562–7

Herculano-Houzel S, Collins CE, Wong P, Kaas JH

Table 1. Comparative cellular composition of the brain of the tree shrew and six primate species

Species	Body mass, g	Brain mass, g	Total neurons, $\times 10^6$	Total nonneurons, $\times 10^6$
Tree shrew	172.5 ± 3.5	2.752 ± 0.011	261.40	199.65
Marmoset	361.0 ± 1.4	7.780 ± 0.654	635.80 ± 115.73	590.74 ± 70.81
Galago	946.7 ± 102.6	10.150 ± 0.060	936.00 ± 115.36	666.59 ± 63.50
Owl monkey	925.0 ± 35.4	15.730	1,468.41	1,195.13
Squirrel monkey	n.a.	30.216	3,246.43	2,075.03
Capuchin monkey	3,340.0	52.208	3,690.52	3,297.74
Macaque monkey	3,900.0	87.346	6,376.16	7,162.90
Variation, macaque/marmoset	10.8×	11.2×	10.0×	12.1×

Species ordered by increasing brain size. Values are mean ± SD. n.a., not available.

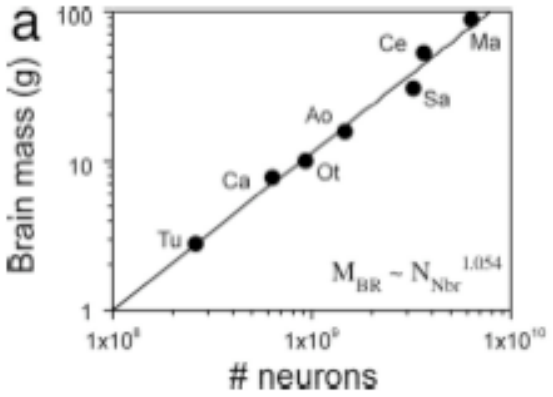

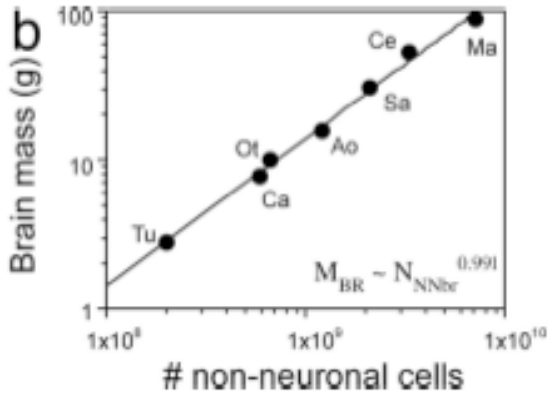

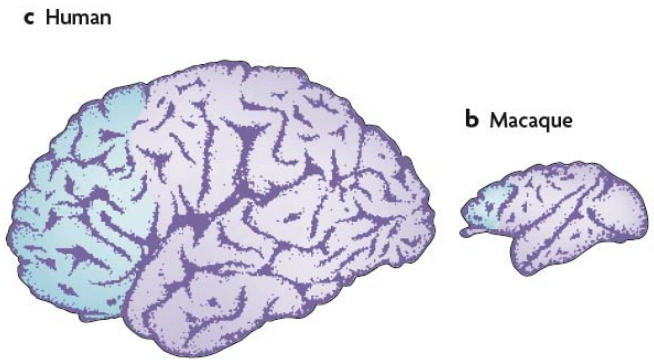

Evolution of increased glia–neuron ratios in the human frontal cortex

Proc Natl Acad Sci USA
2006 vol. 103 (37) pp. 13606–11

Sherwood CC, Stimpson CD, Raghanti MA, Wildman DE, Uddin M, Grossman LI, Goodman M, Redmond JC, Bonar CJ, Erwin JM, Hof PR

Table 1. Brain weights and glia–neuron ratios for layer II/III of prefrontal area 9L (species mean)

Species	*n*	Brain weight, g	Glia–neuron ratio
Homo sapiens	6	1,373.3	1.65
Pan troglodytes	6	336.2	1.20
Gorilla gorilla	2	509.2	1.21
Pongo pygmaeus	2	342.7	0.98
Hylobates muelleri	1	101.8	1.22
Papio anubis	2	155.8	0.97
Mandrillus sphinx	1	159.2	1.02
Macaca maura	6	92.6	0.84
Erythrocebus patas	2	102.3	1.09
Cercopithecus kandti	1	71.6	1.15
Colobus angolensis	1	74.4	1.20
Trachypithecus francoisi	1	91.2	1.14
Alouatta caraya	1	55.8	1.12
Saimiri boliviensis	1	24.1	0.51
Aotus trivirgatus	1	13.2	0.63
Saguinus oedipus	1	10.0	0.46
Leontopithecus rosalia	2	12.2	0.60
Pithecia pithecia	1	30.0	0.64

Evolution of increased glia–neuron ratios in the human frontal cortex

Proc Natl Acad Sci USA
2006 vol. 103 (37) pp. 13606–11

Sherwood CC, Stimpson CD, Raghanti MA, Wildman DE, Uddin M, Grossman LI, Goodman M, Redmond JC, Bonar CJ, Erwin JM, Hof PR

Table 2. Glia–neuron ratios in layer II/III of different areas in frontal cortex

Species	*n*	Area 4	Area 9L	Area 32	Area 44
Homo sapiens	6	2.19 (0.06)	1.65 (0.09)	1.63 (0.09)	1.55 (0.18)
Pan troglodytes	6	1.54 (0.05)	1.20 (0.06)	0.91 (0.09)	1.24 (0.13)
Macaca maura	6	1.29 (0.09)	0.84 (0.03)	0.68 (0.05)	0.95 (0.06)

Data are presented as mean (standard error).

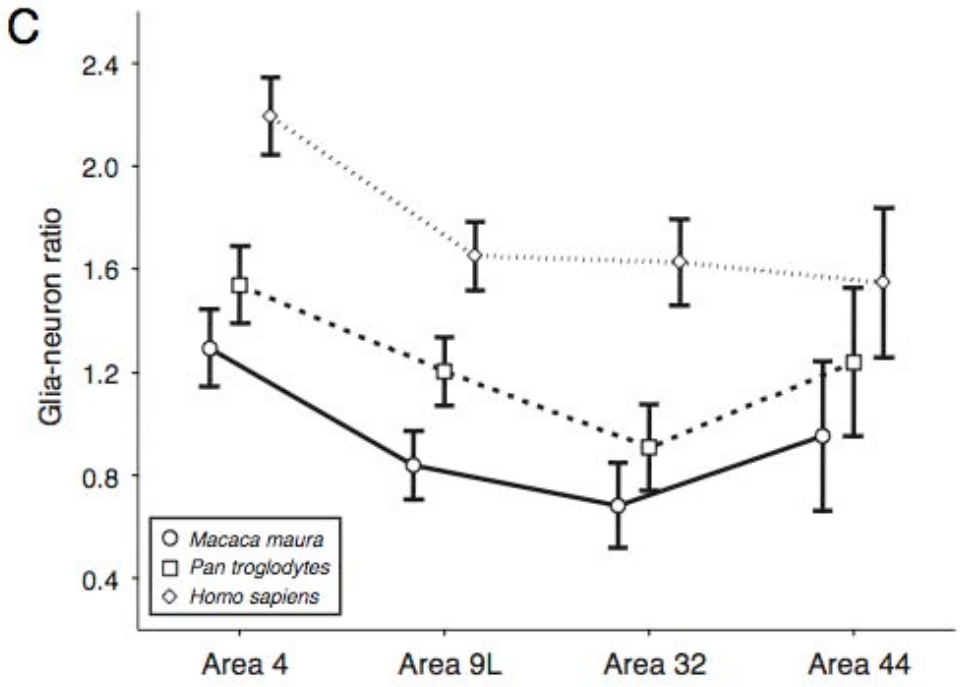

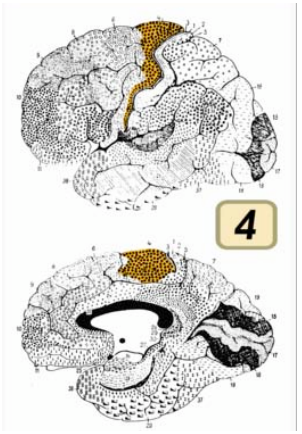

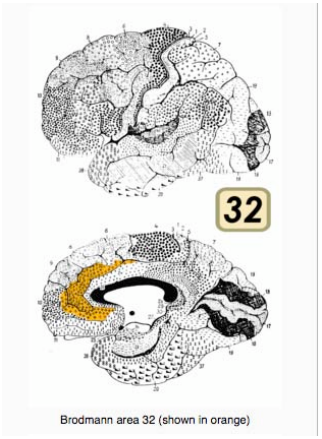

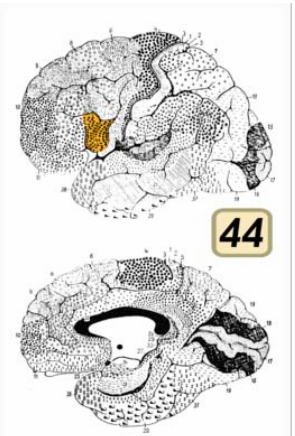

Evolution of the neocortex: a perspective from developmental biology

Rakic P

Nat Rev Neurosci
2009 vol. 10 (10) pp. 724-35

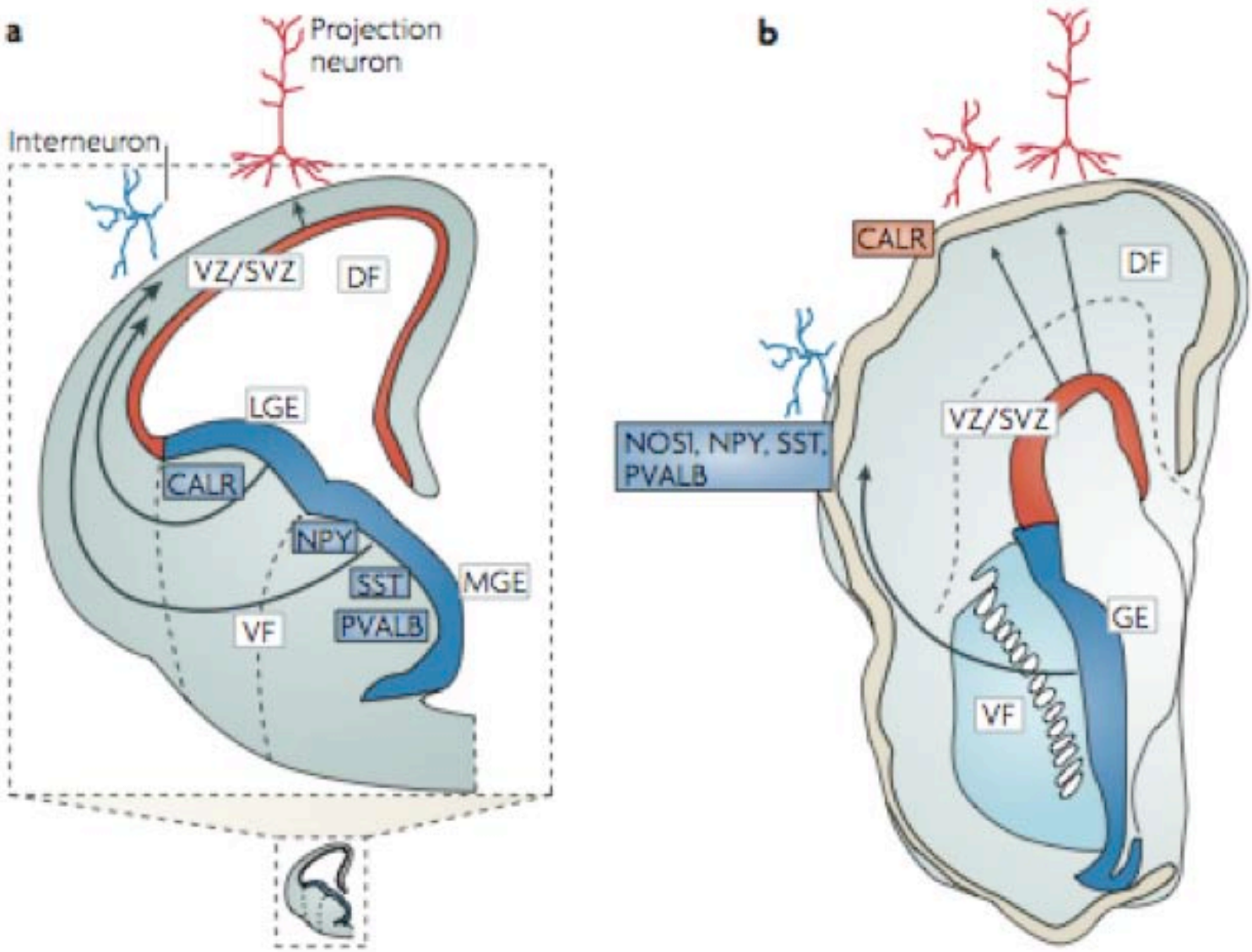

CRITICAL PERIOD AND MATURATION OF LOCAL GABAERGIC CIRCUITS

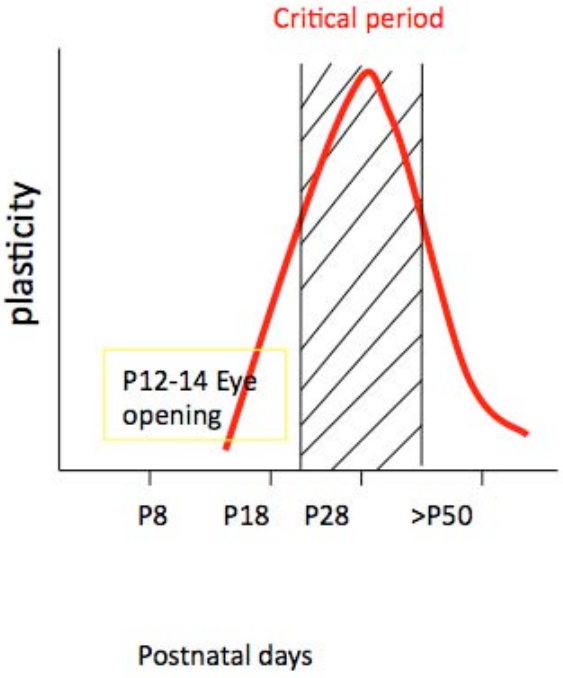

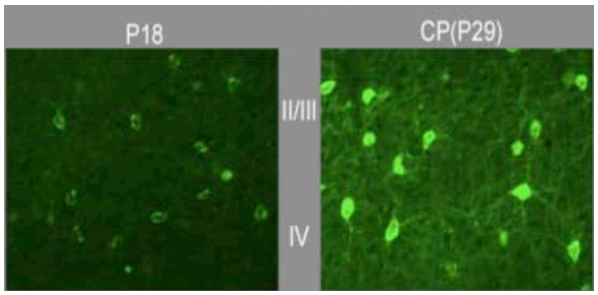

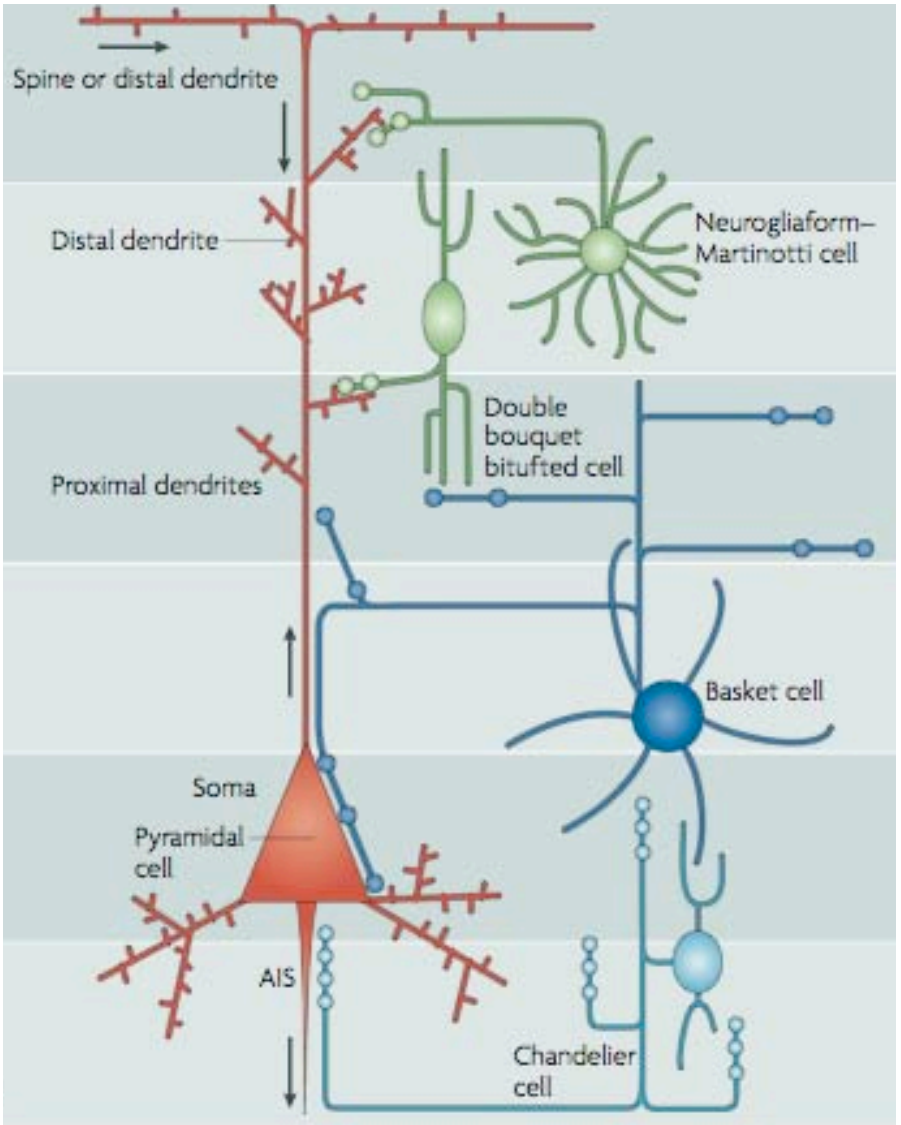

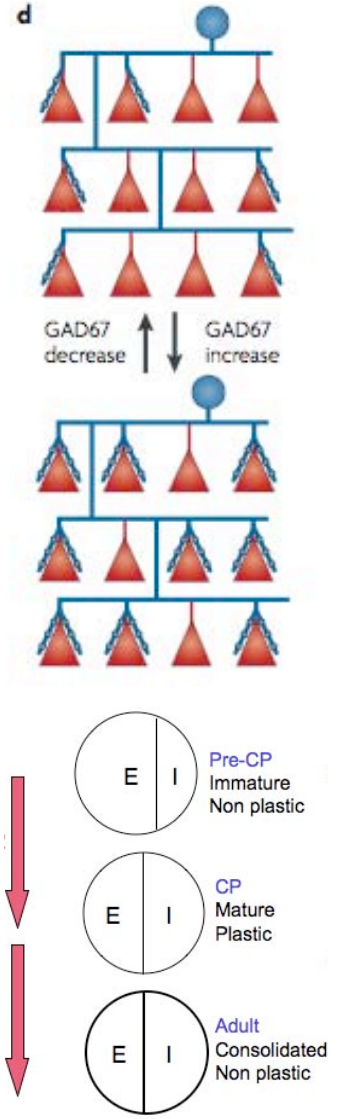

OPINION

Why do many psychiatric disorders emerge during adolescence?

Tomáš Paus, Matcheri Keshavan and Jay N. Giedd

NATURE REVIEWS | NEUROSCIENCE

VOLUME 9 | DECEMBER 2008 |

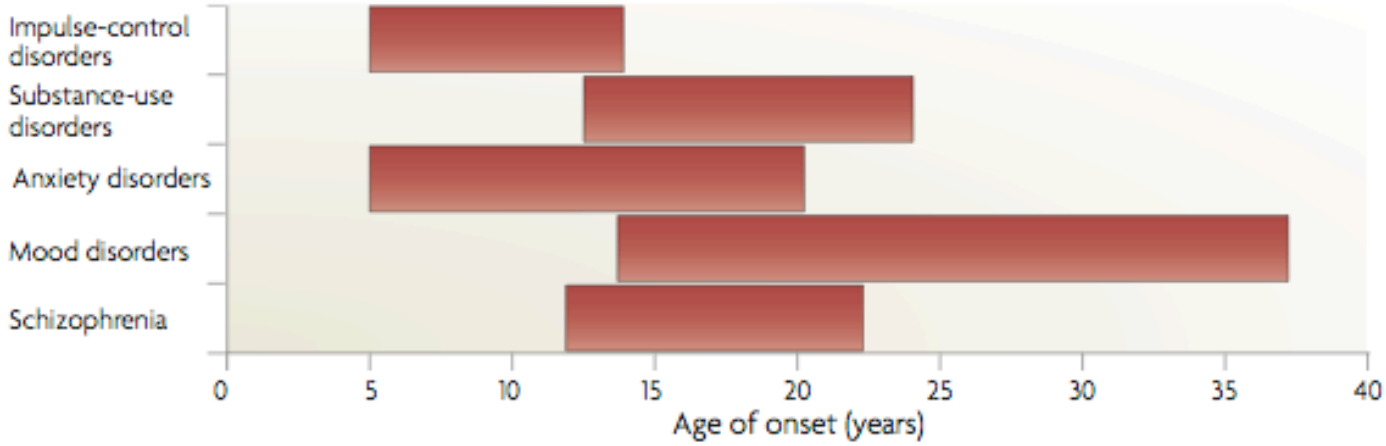

Reversing Neurodevelopmental Disorders in Adults

Dan Ehninger,[1] Weidong Li,[1] Kevin Fox,[2] Michael P. Stryker,[3] and Alcino J. Silva[1,*]
[1]Departments of Neurobiology, Psychiatry and Biobehavioral Sciences, Psychology and the Brain Research Institute, University of California, Los Angeles, 695 Charles Young Drive South, Los Angeles, CA 90095-1761, USA
[2]Cardiff School of Biosciences, Cardiff University, Museum Avenue, Cardiff CF10 3US, UK
[3]Department of Physiology, W.M. Keck Foundation Center for Integrative Neuroscience, University of California, San Francisco, San Francisco, CA 94143-0444, USA
*Correspondence: silvaa@ucla.edu
DOI 10.1016/j.neuron.2008.12.007

Rethinking schizophrenia

Thomas R. Insel[1]

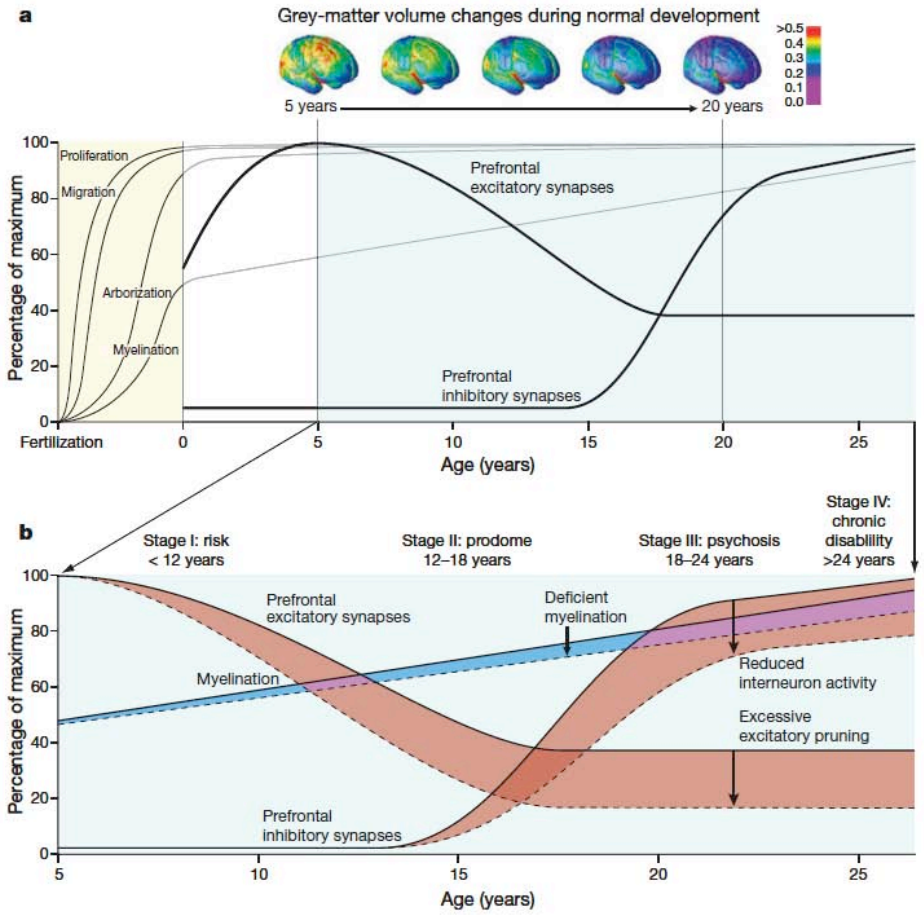

THE MAKING OF A TROUBLED MIND

BY DAVID DOBBS

ACCENT ON YOUTH

Distribution of age at first admission for schizophrenia in males and females.

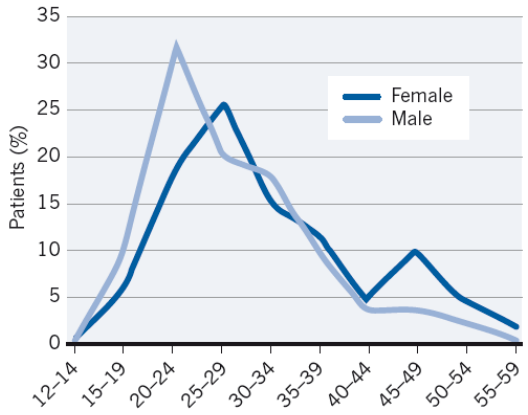

Figure 1 | Neurodevelopmental model of schizophrenia. **a**, Normal cortical development involves proliferation, migration, arborization (circuit formation) and myelination, with the first two processes occurring mostly during prenatal life and the latter two continuing through the first two post-natal decades. The combined effects of pruning of the neuronal arbor and myelin deposition are thought to account for the progressive reduction of grey-matter volume observed with longitudinal neuroimaging. Beneath this observed overall reduction, local changes are far more complex. Data from human and non-human primate brain indicate increases in inhibitory and decreases in excitatory synaptic strength occurring in prefrontal cortex throughout adolescence and early adulthood, during the period of prodrome and emergence of psychosis. **b**, The trajectory in children developing schizophrenia could include reduced elaboration of inhibitory pathways and excessive pruning of excitatory pathways leading to altered excitatory–inhibitory balance in the prefrontal cortex. Reduced myelination would alter connectivity. Although some data support each of these possible neurodevelopmental mechanisms for schizophrenia, none has been proven to cause the syndrome. Detection of prodromal neurodevelopmental changes could permit early intervention with potential prevention or preemption of psychosis.

A Resource for Transcriptomic Analysis in the Mouse Brain

Charles Plessy[1], Michela Fagiolini[2], Akiko Wagatsuma[2], Norihiro Harasawa[3], Takenobu Kuji[2], Atsuko Asaka-Oba[2], Yukari Kanzaki[2], Sayaka Fujishima[2], Kazunori Waki[4], Hiroyuki Nakahara[3], Takao K. Hensch[2]*, Piero Carninci[1]*

August 2008 | Volume 3 | Issue 8 | e3012

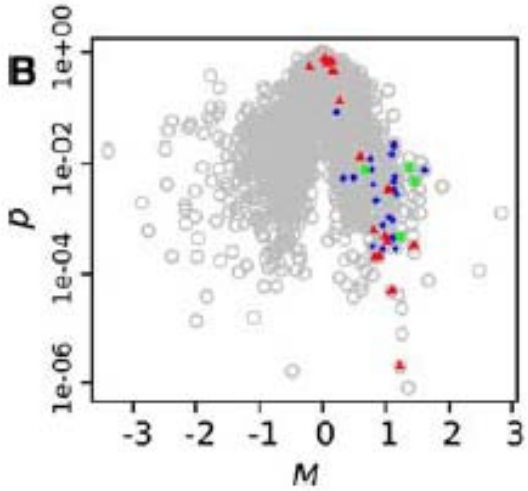

Blue diamond: Nduf family
Red triangles: Atp5 family
Green dots: Cox6 family

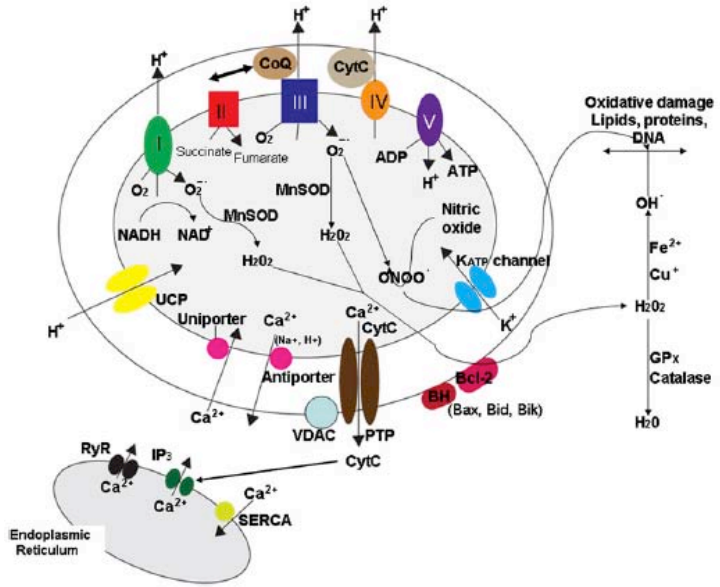

CLONE_ID	SYMBOL	p	M
K230031N16	Ndufa11	7.69E-3	1.61
K230002F10	Cox6c	4.77E-3	1.46
K330002E13	Atp5g3	3.25E-4	1.44
K230006O16	Cox6c	8.83E-3	1.37
K230309I10	Cox6b1	4.73E-4	1.22
K230001M19	Atp5h	1.99E-6	1.22
K230340G22	Ndufb9	2.84E-3	1.16
K230002E05	Ndufb8	2.84E-4	1.15
K230006I15	Ndufa8	5.80E-3	1.14
K230009H06	Ndufs5	3.36E-3	1.13
K230012O10	Ndufa2	2.13E-2	1.13
K230310N23	Ndufb7	9.34E-4	1.11
K330022I20	Ndufa6	4.48E-4	1.11
K230010M09	Atp5h	4.84E-5	1.09
K230310M07	Ndufa5	1.50E-2	1.09
K230044G12	Ndufc2	1.06E-3	1.06
K230319K23	Atp5g1	3.37E-3	1.04
K230012P07	Atp5j	3.80E-4	1.02
K230304A02	Ndufa5	8.35E-3	0.96
K230019O17	Ndufs2	2.80E-4	0.95
K230304I19	Ndufb10	7.66E-4	0.95
K330018J12	Atp5e	1.94E-3	0.92
K230039K18	Atp5c1	2.06E-4	0.89
K230050F20	Ndufb2	2.15E-3	0.85
K230053K02	Atp5o	1.98E-4	0.83
K230014B16	Atp5c1	6.17E-4	0.81
K230003F11	Ndufs8	4.23E-3	0.80
K230304N08	Ndufv2	3.12E-4	0.79
K330022A12	Ndufv1	7.91E-3	0.78
K230008K02	Ndufa10	1.25E-2	0.76
K230001C13	Cox6a1	7.63E-3	0.66
K330009A17	Atp5d	1.36E-2	0.60
K230053L04	Ndufs3	5.61E-3	0.49
K230005J19	Ndufaf1	5.43E-3	0.32
K230034B16	Atp5g2	1.27E-1	0.27
K230003B02	Ndufs1	8.05E-2	0.22
K230003P04	Atp5f1	4.42E-1	0.16
K230018C04	Atp5b	6.76E-1	0.14
K230001F17	Atp5a1	6.43E-1	0.07
K230302C16	Atp5s	7.52E-1	0.04
K230001C22	Atp5b	5.26E-1	−0.21

A novel (ancient?) signaling mechanism

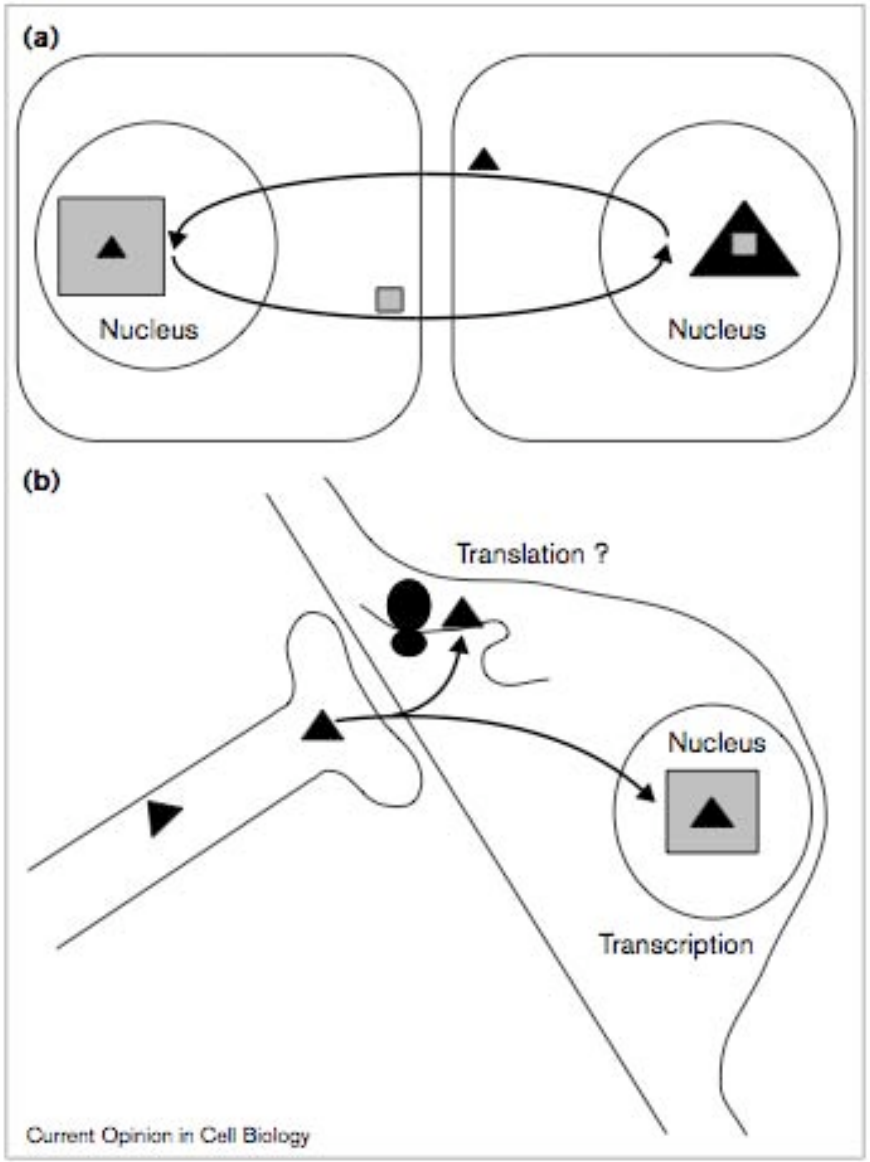

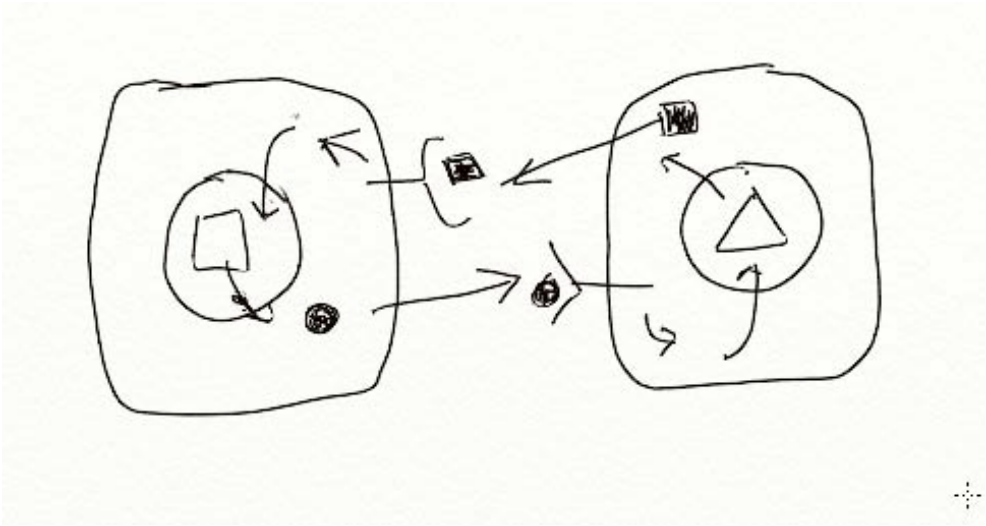

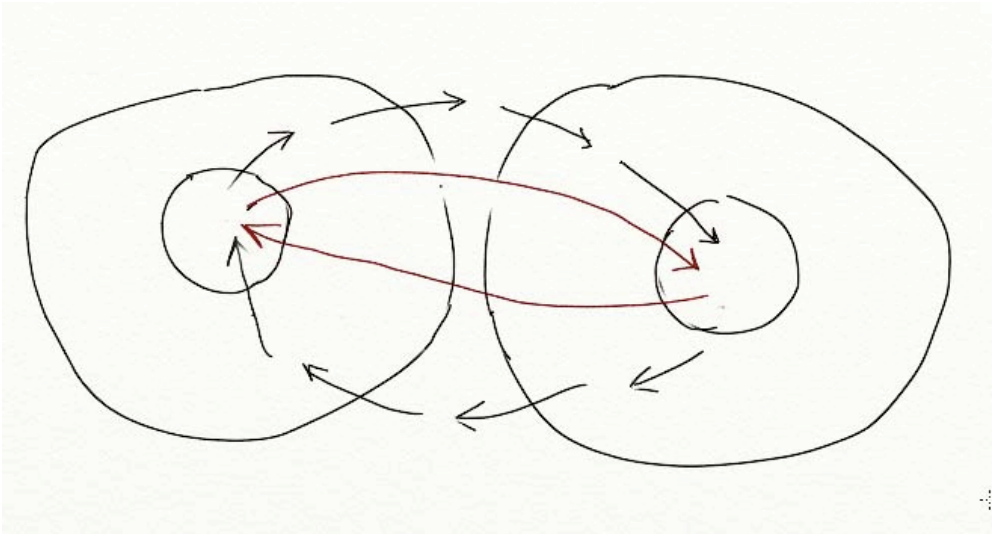

Central visual pathway and critical period for binocular vision

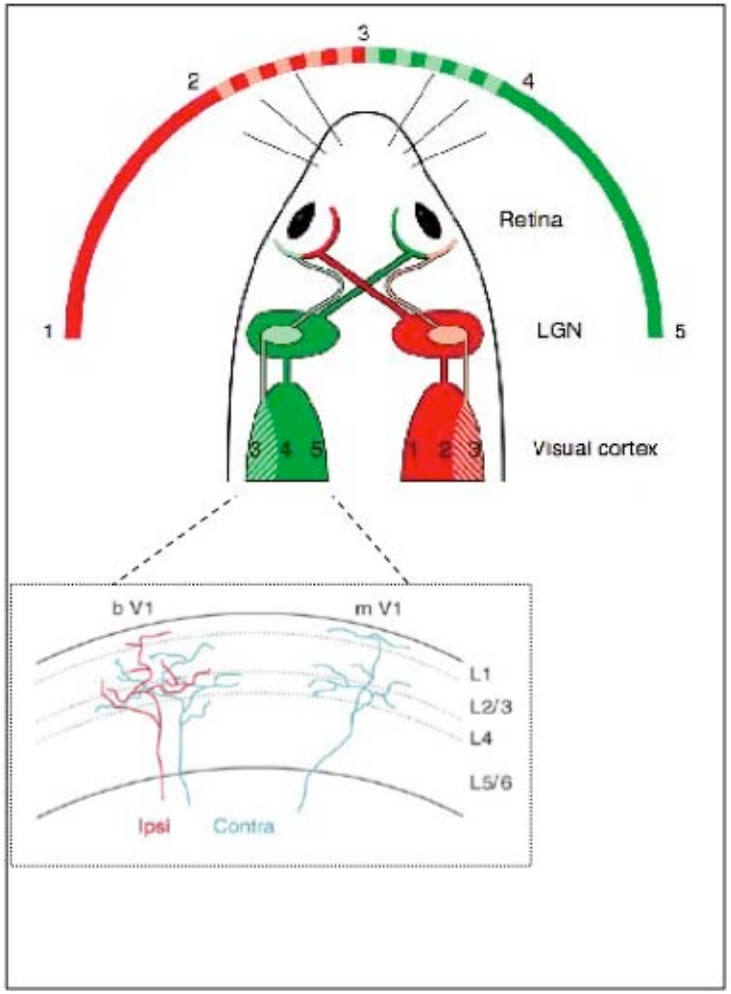

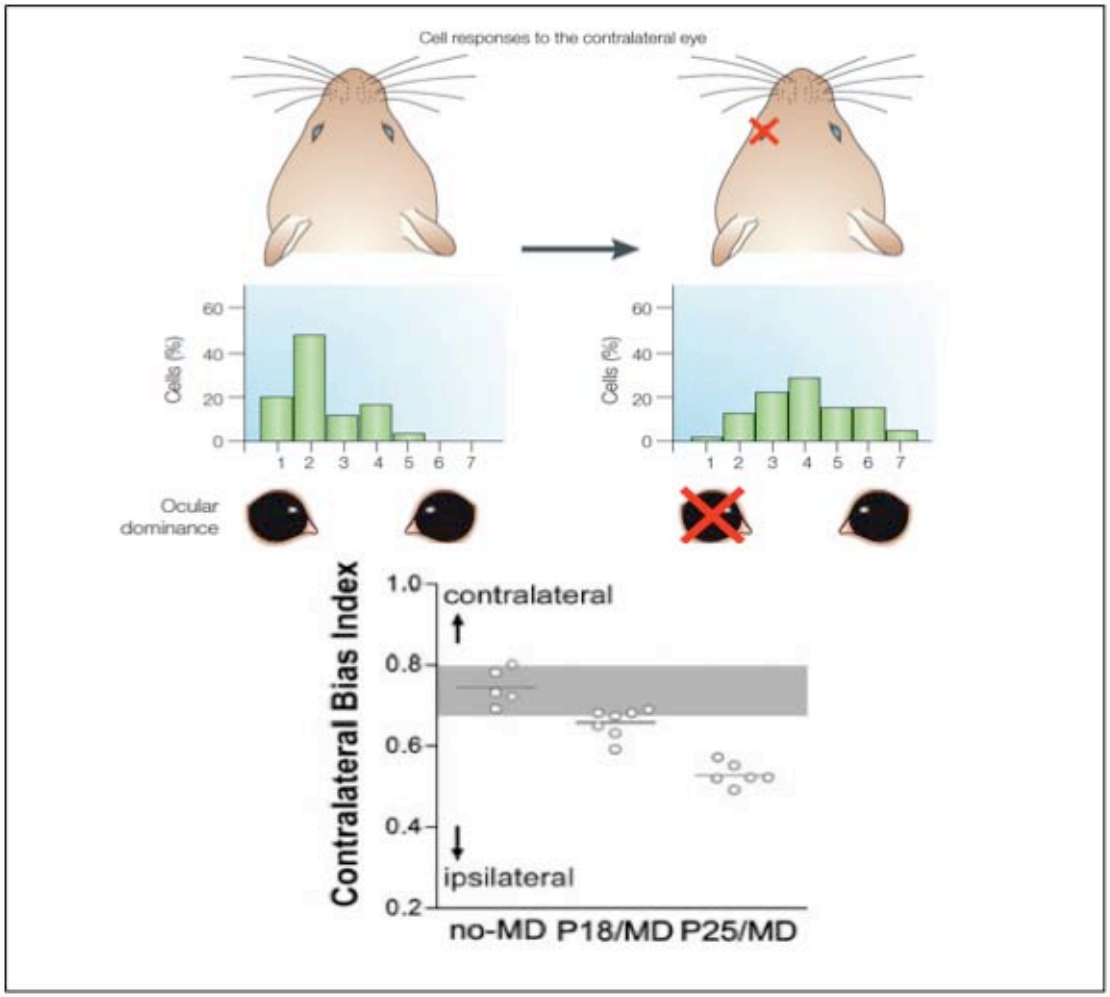

Otx2 expression in PV cells parallels critical period

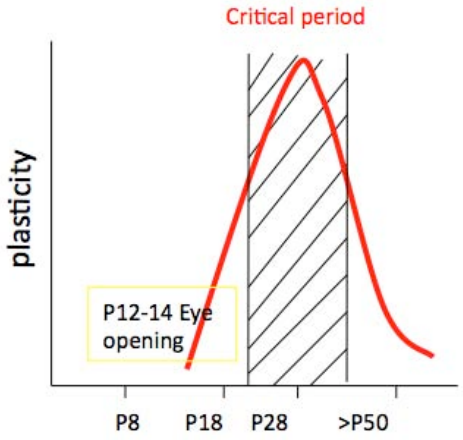

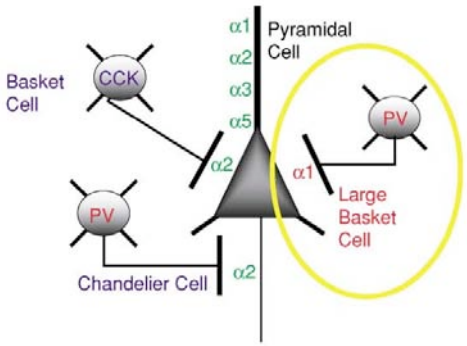

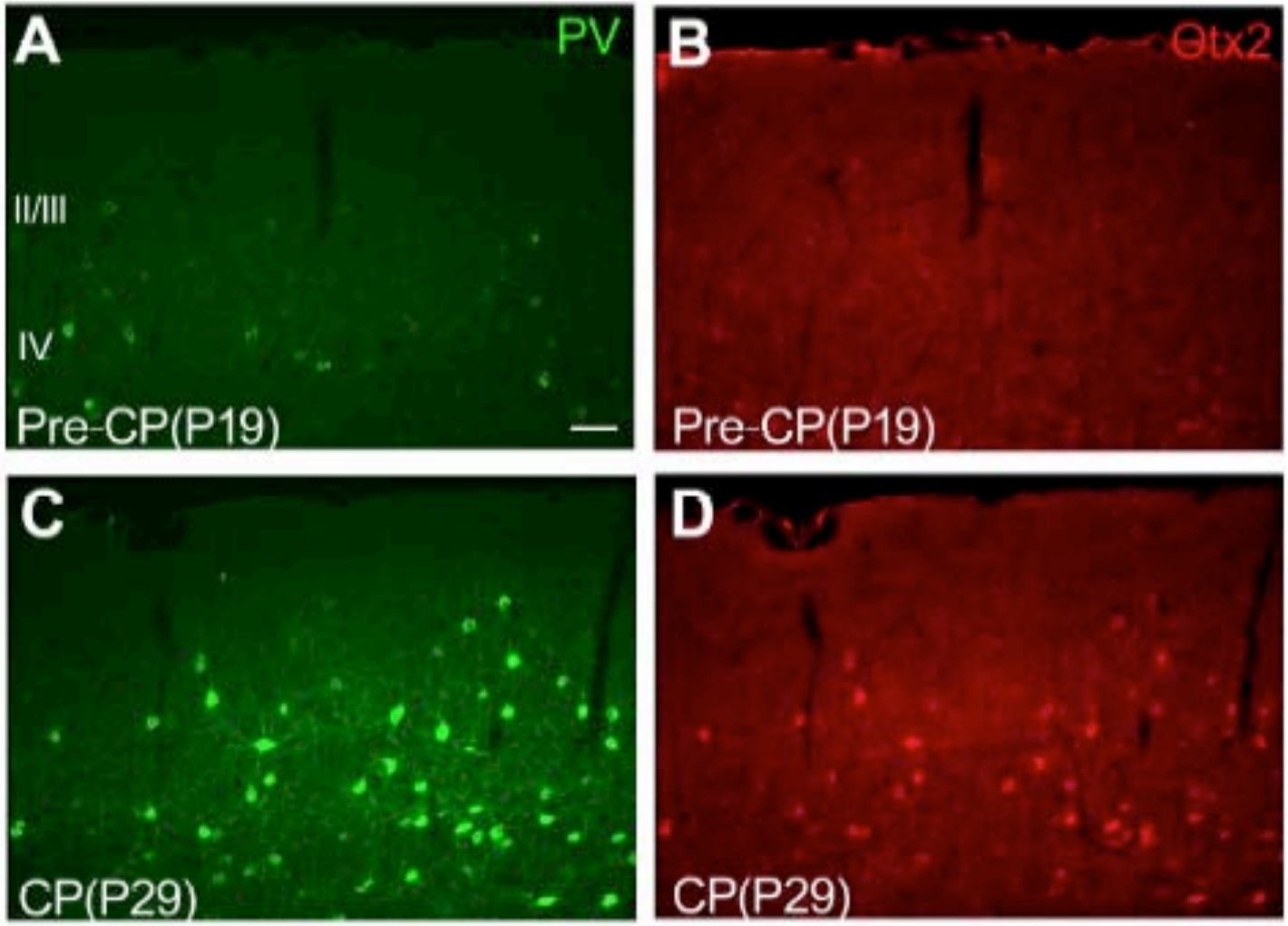

Sugiyama et al. *Cell* 2008

Otx2 expression, as PV maturation, is activity-dependent

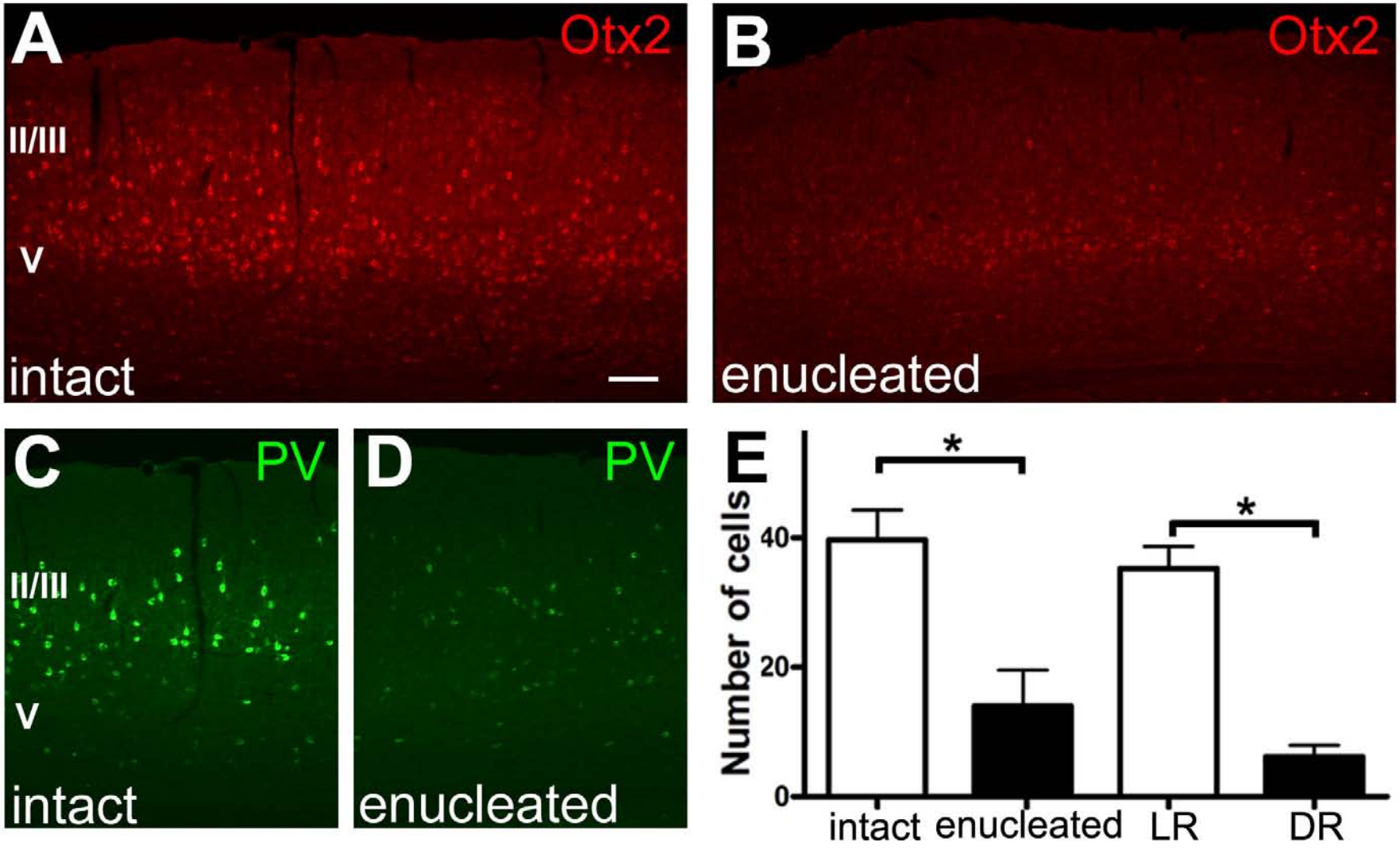

Sugiyama et al. *Cell* 2008

AN OTX2 MOTIF IS NECESSARY FOR ITS BINDING TO CORTICAL CELLS

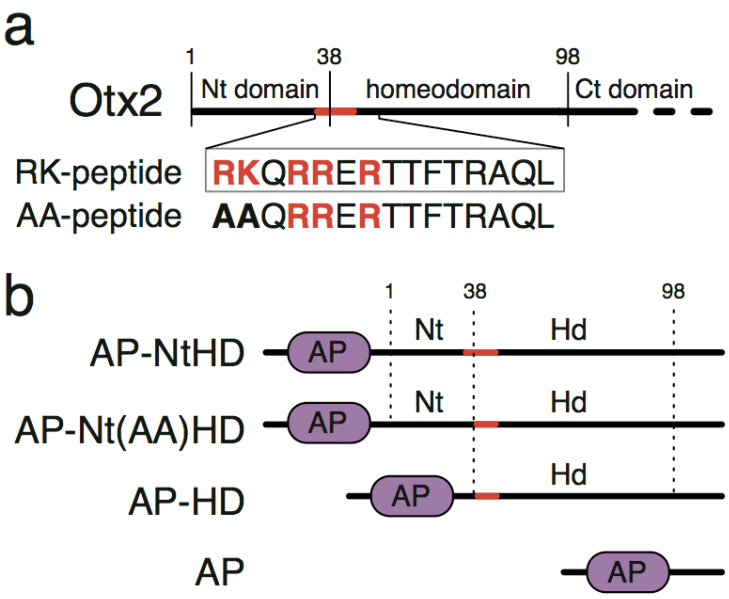

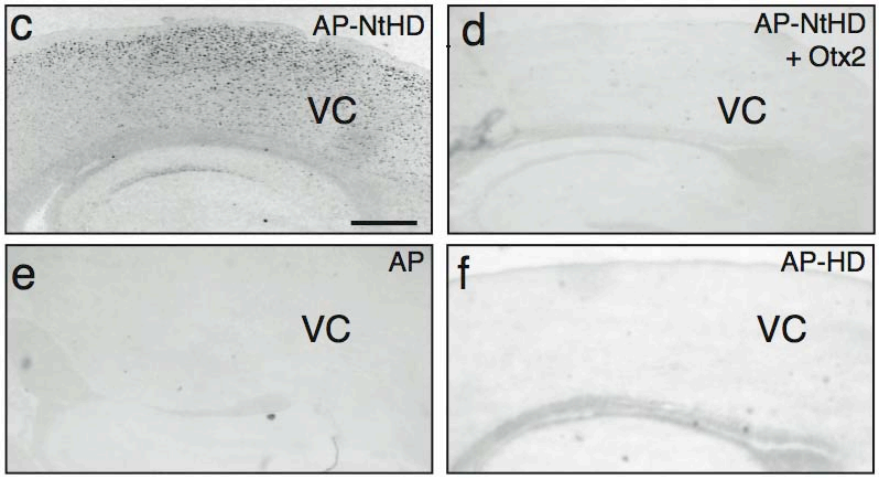

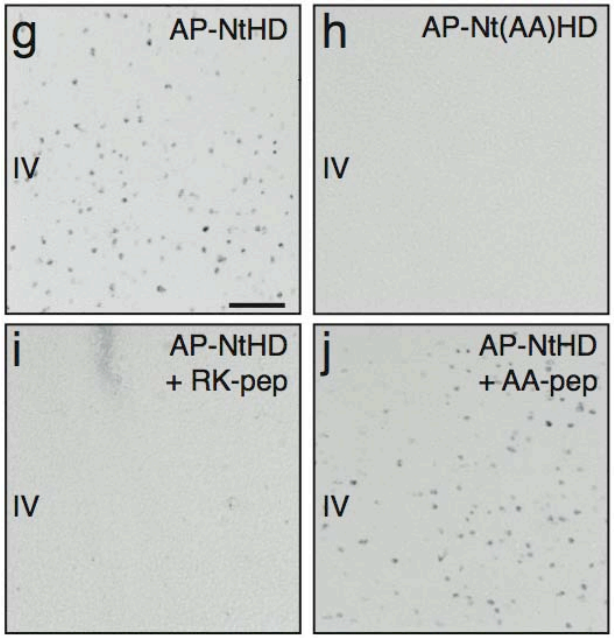

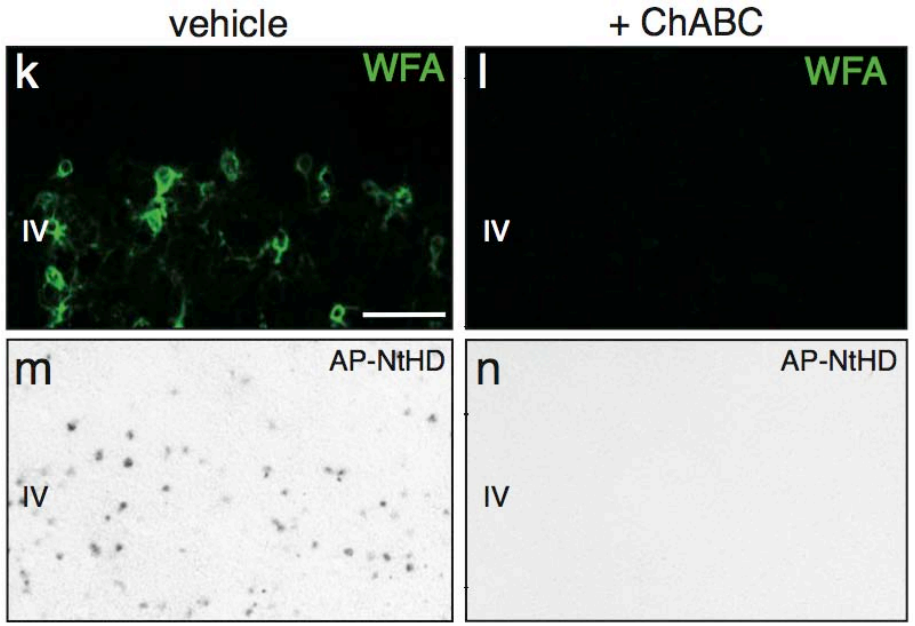

RK-PEPTIDE INFUSION IMPAIRS ENDOGENOUS OTX2 TRANSFER INTO V1

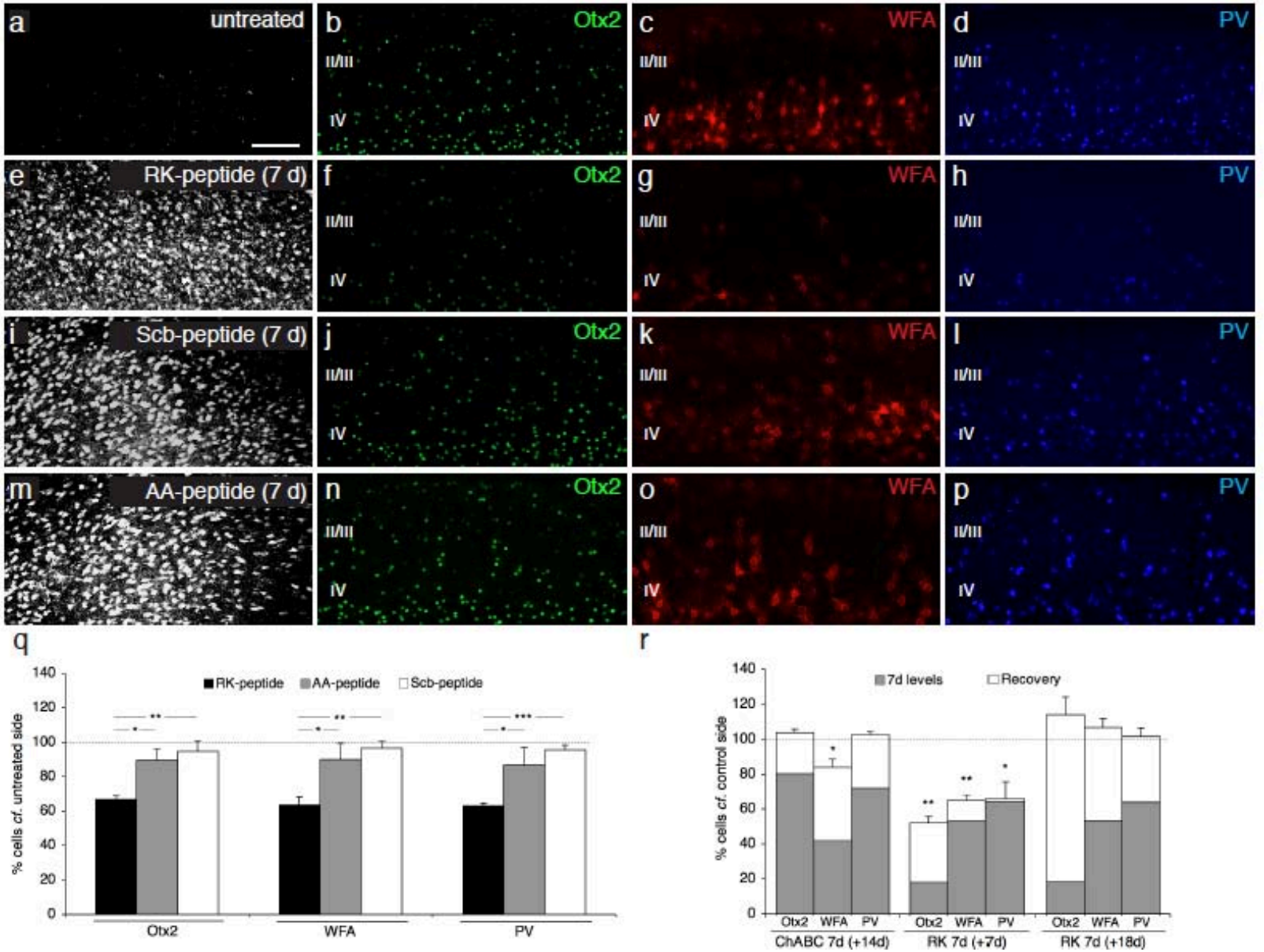

Beurdeley, Spatazza et al., in revision

RK-PEPTIDE REOPENS PLASTICITY IN THE ADULT

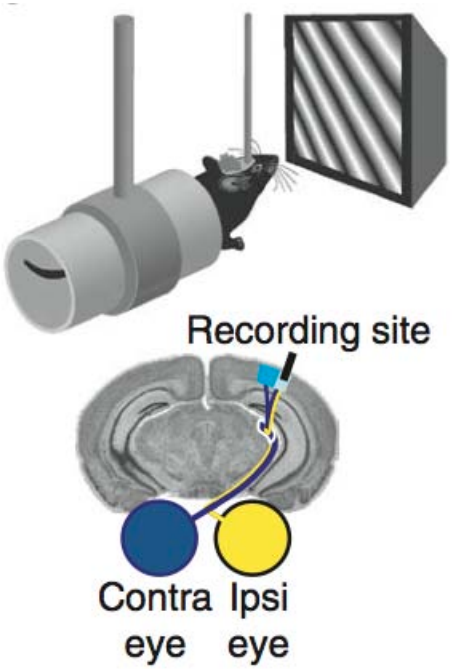

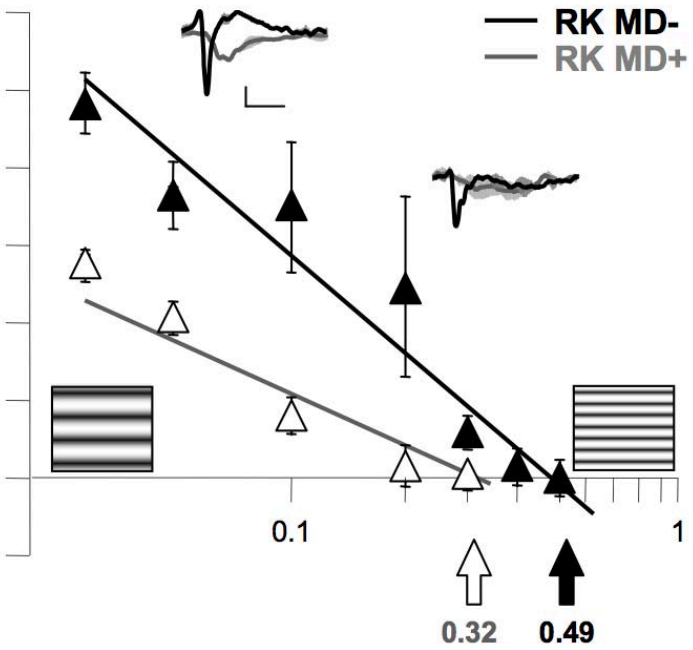

Recording

STMD

> P 60

D0 D2 D6 D7

Normal adult mouse visual acuity : ≈ 0,45 – 0,6

Beurdeley, Spatazza et al., in revision

RECOVERY FROM AMBLYOPIA

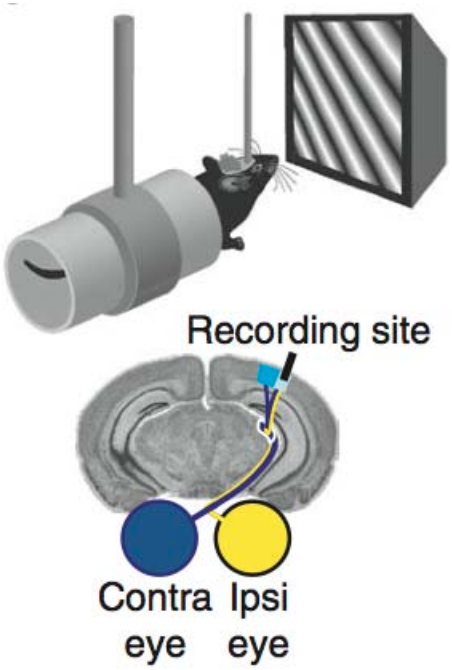

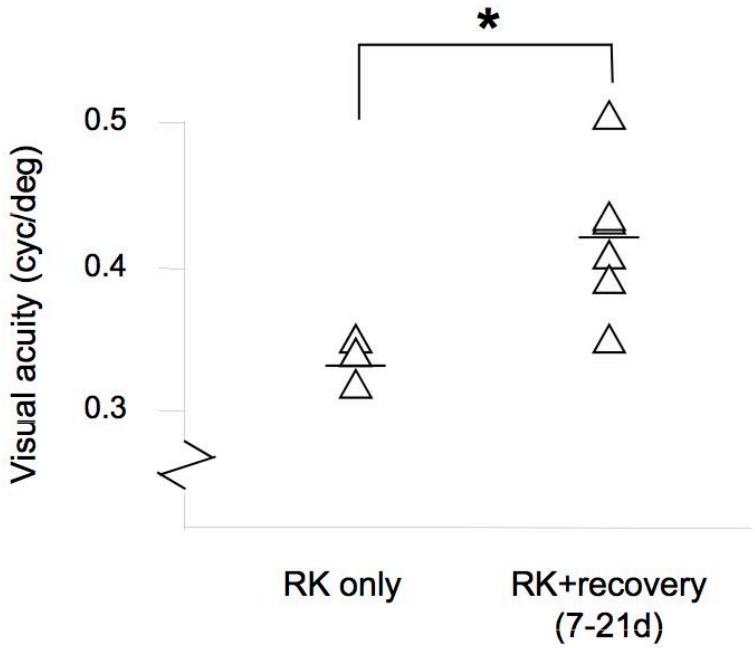

Recording Recording

LTMD Infusion

P19 P33 P60 P67 P74-95

Otx2 is expressed in the choroid plexus where it can be specifically recombined

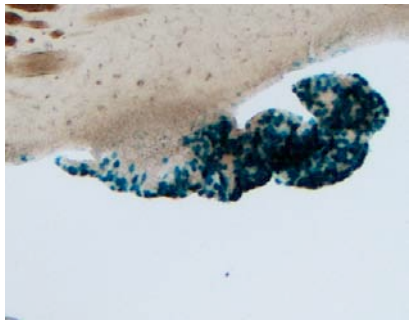

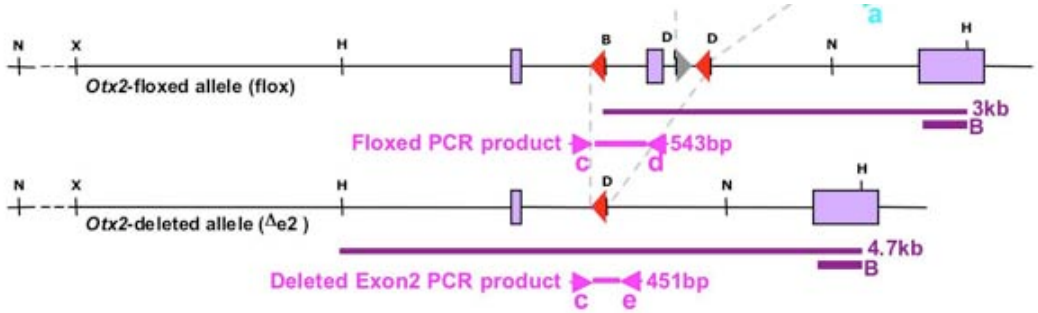

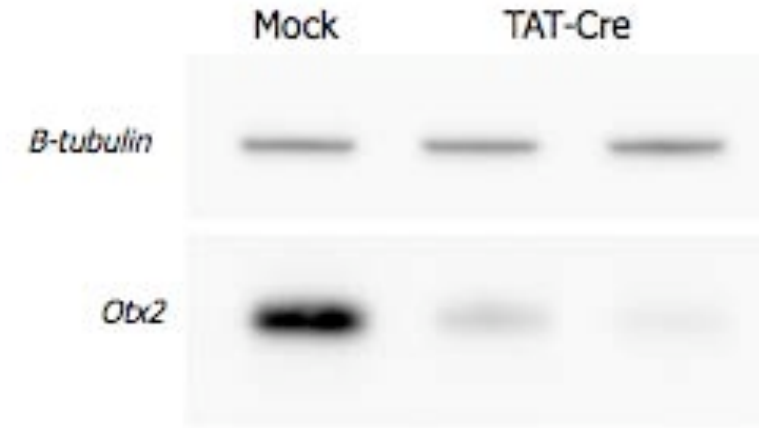

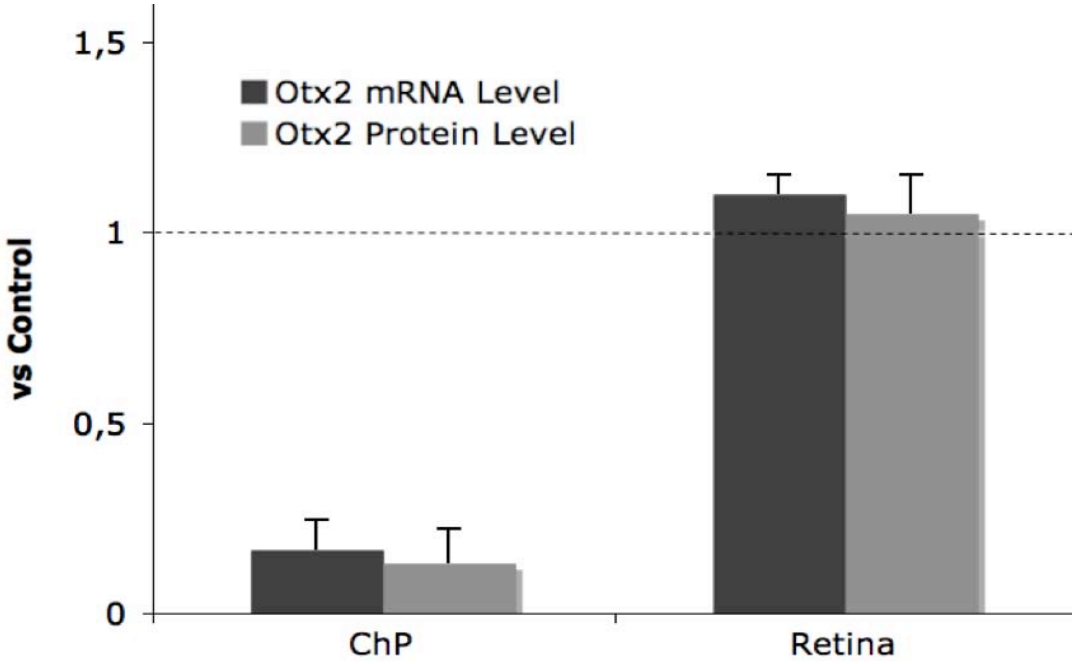

Spatazza et al. in preparation

RECOMBINING OTX2 IN THE CHOROID PLEXUS REDUCES ITS CORTICAL CONTENT AND REDUCES PV CELL MATURATION MARKERS

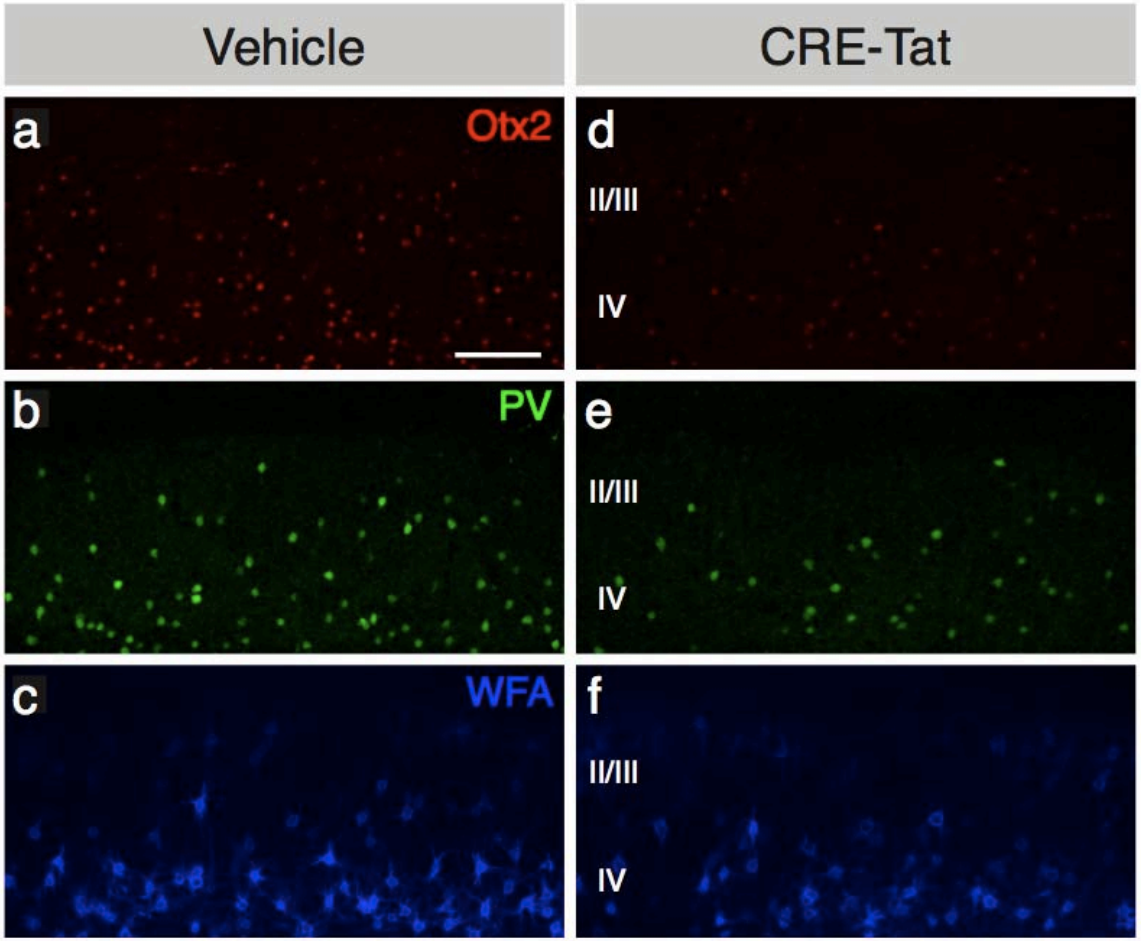

Sacrifice 14 days after a single CRE-Tat injection

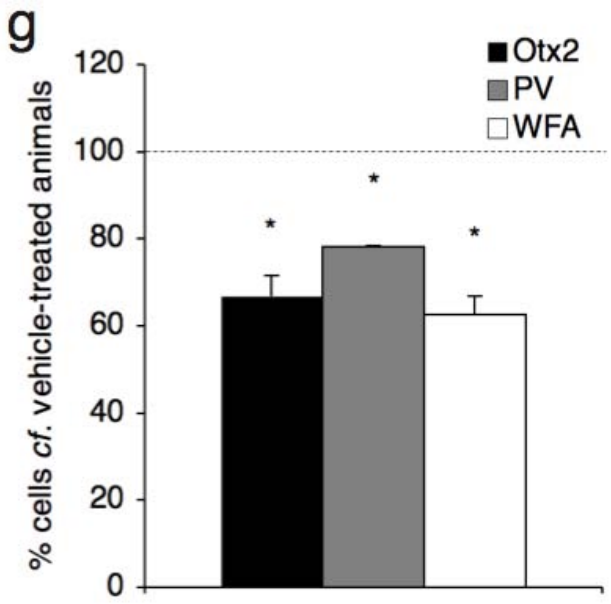

RECOMBINING OTX2 IN THE ADULT PLEXUS REOPENS PLASTICITY